

APPROVAL SHEET

Title of Thesis: Analysis of Low-Cost Particulate Matter Shinyei Sensor for
Asthma Research

Name of Candidate: Robert K Burton
Master of Science, 2017

Thesis and Abstract Approved: _____

Christopher Hennigan, Ph.D.
Assistant Professor
Chemical, Biochemical, and Environmental
Engineering

Date Approved: _____

ABSTRACT

Title of Document: Analysis of Low-Cost Particulate Matter Shinyei Sensor for Asthma Research

Robert Kentucky Burton, Master of Science,
2017

Directed By: Christopher Hennigan, Ph.D., Assistant Professor, Chemical, Biochemical, and Environmental Engineering

Asthma is a prevalent chronic respiratory ailment which affects 7.1 million children in the United States. Asthma is aggravated by environmental and physiological factors, including air pollutants such as particulate matter. Particulate matter includes solid and liquid particles suspended in the air, such as pollen, dust, dander, and smoke. This research contributes to the development of a low-cost, low-power particulate matter sensor. The particulate matter sensor will aid in the determination of the triggers for asthma by allowing for more accurate identification of particle concentration, size, and type. This project involved a detailed characterization of the Shinyei PD42NS particle sensor. The particle sensor uses a process known as nephelometry, light scattering, to measure the particle concentration. The sensor performance was characterized for varying particle types and sizes, including sodium chloride (NaCl), polystyrene latex (PSL) microspheres, and incense smoke. Modifications to the sensor by changing the LED type, increasing the air flow rate, and lowering the threshold of detection were investigated. Ultimately, this work will

inform the development of a new low-cost, wearable PM sensor that will be deployed for pediatric asthma research.

ANALYSIS OF LOW-COST PARTICULATE MATTER SHINYEI SENSOR FOR
ASTHMA RESEARCH

By

Robert Kentucky Burton

Thesis submitted to the Faculty of the Graduate School of the
University of Maryland, Baltimore County, in partial fulfillment
of the requirements for the degree of
Master of Science
2017

© Copyright by
Robert Kentucky Burton
2017

Acknowledgements

I would like to thank my advisors, Dr. Christopher Hennigan and Dr. Yordan Kostov, the CBEE faculty and students, and my family and friends.

Table of Contents

Acknowledgements.....	ii
Table of Contents.....	iii
List of Tables.....	iv
List of Figures.....	v
1.0 Introduction.....	1
2.0 Background.....	5
2.1 Particulate Matter.....	5
2.1.1 Sources of Particulate Matter.....	5
2.1.2 Regulatory Standards.....	6
2.1.3 Ambient Particulate Matter Concentrations.....	6
2.1.4 Particulate Matter size distributions.....	7
2.1.5 Health Effects of Particulate Matter.....	7
2.2 Microenvironments.....	9
2.3 Nephelometry.....	10
2.3.1 Mie Theory.....	12
2.4 Low-Cost Sensors.....	14
2.4.1 Shinyei.....	16
3.0 Methods.....	18
3.1 Shinyei PD42NS.....	18
3.2 Shinyei PD42NS UMBC Prototypes.....	19
3.3 Particulate types.....	21
3.4 Experimental Set-up.....	23
3.4.1 Shinyei Sensor Unit/ Arduino Microcontroller test device.....	27
3.4.2 DustTrak II Aerosol Monitor.....	28
3.5 Experimental Test Series.....	28
4.0 Results and Discussion.....	29
4.1 Shinyei PD42NS Characterization.....	29
4.2 Prototype-G – LED Wavelength Variation.....	39
4.3 Prototype-R – Potentiometer improvements.....	43
4.4 Flowrate Comparisons.....	48
4.5 Variation with Time.....	50
4.6 Simulation results.....	51
5.0 Conclusion.....	54
5.1 Future Work.....	56
References.....	59

List of Tables

Table 2.1: Particulate Matter Ambient Regulations	6
Table 2.2: Sample Refractive Indexes	12
Table 2.3: Regression Closeness of Fit for various PM Sensors	15
Table 3.1: Prototype Modifications	19
Table 3.2: Average readings and standard deviation of dynamic blanks	27
Table 3.3: Experimental Test Matrix	28
Table 4.1: Parameters varied in the Mie simulations.....	51

List of Figures

Figure 3.1: Piezo pump flow calibration as a function of input voltage.....	21
Figure 3.2: Relationship between aqueous NaCl concentration and particle size generated by the atomizer.	22
Figure 3.3: Experimental setup for an incense test.	23
Figure 3.4: Schematic showing PM generation for NaCl and PSL tests.	25
Figure 3.5: Dynamic blank timeseries	26
Figure 4.1: Unmodified Shinyei PD42NS & DustTrak II Time Series for experiment with 0.25 M NaCl	30
Figure 4.2: Shinyei calibration – 0.25 M NaCl.....	30
Figure 4.3: Shinyei PD42NS calibration non-saturated region – 0.25 M NaCl	31
Figure 4.4: Shinyei PD42NS calibration series – NaCl (one point from the 0.5 M NaCl series is off the graph)	32
Figure 4.5: Unmodified Shinyei PD42NS & DustTrak II Time Series for experiment with 2 μ m PSL	33
Figure 4.6: Shinyei PD42NS calibration series – Polystyrene Latex microspheres ...	33
Figure 4.7: Shinyei PD42NS calibration series – Incense	34
Figure 4.8: Shinyei PD42NS vs. DustTrak slope	35
Figure 4.9: Shinyei PD42NS vs. DustTrak R^2 values.....	38
Figure 4.10: Green vs Infrared time series – 0.1 M NaCl.....	40
Figure 4.11: Shinyei vs DustTrak – 0.1 M NaCl	40
Figure 4.12: Infrared Shinyei output vs green Shinyei output comparison – 0.1 M NaCl	41
Figure 4.13: Infrared Shinyei output vs green Shinyei output comparison – 1 μ m PSL	41
Figure 4.14: Compilation of green response to infrared response – NaCl.....	42
Figure 4.15: Prototype – R 15 k Ω and DustTrak time series – 1 μ m PSL	44
Figure 4.16: DustTrak vs Prototype – R 15 k Ω - 1 μ m PSL.....	44
Figure 4.17: Prototype-R response in relation to resistance change – 1 μ m PSL microspheres	45
Figure 4.18: P1 vs P2 1 μ m PSL – red 5 k Ω ; black 15 k Ω	46
Figure 4.19: PSL Sensitivity Ratio in relation to effective Potentiometer Resistance	46
Figure 4.20: Time series of the experiment run with 2 μ m PSL to compare the Shinyei response under different flow configurations.	49
Figure 4.21: Variation in response with time – 1 μ m PSL	50
Figure 4.22: Variation in scattering intensity over scattering angle and refractive index.....	52
Figure 4.23: Variation in scattering intensity over scattering angle and wavelength.	52

1.0 Introduction

Pediatric Asthma is a major health problem in the United States, affecting ~8-9 percent of children.¹ There are many phenotypes of asthma which each have their own environmental triggers and management plans. Phenotypes are classified by the severity of the symptoms, the frequency of the symptoms, the age of onset, and the triggers of symptoms. Even in pediatric asthma, there are many different types and proper identification is crucial for proper treatment.² Pediatric asthma is often allergenic asthma and has no cure: therefore, the approach to treatment uses symptom management to control the disease. In addition to the use of pharmaceuticals, avoidance of allergens and air pollutants are used to mitigate symptoms. Exacerbation of asthma can be life threatening, so it is important to identify risk factors unique to each individual patient.³

Particulate matter (PM) consists of solid and liquid particles suspended in the air. Particulate matter is known to aggravate asthma symptoms.⁴ Also, maternal smoking and exposure to outdoor air pollutants have been identified as increased risk factors for the development of asthma in children.⁵ Particulate matter from traffic has been shown to increase the probability of developing chronic asthma.⁵ Black carbon (pure carbon which comes from incomplete combustion of biomass and fossil fuels), PM_{2.5} (particles with diameters less than 2.5 μm) and PM₁₀ (particles with diameters less than 10 μm) are associated with the development of asthma, as well.⁶

Due to the variability in pediatric asthma phenotypes, the disease is most effectively managed on the individual patient level.⁷ This includes an understanding of the particulate matter types and concentrations that an individual is exposed to

each day. However, the cost of current PM measurement technology precludes such an assessment, given the high number of sensors that would be required. This has motivated the development of new, low-cost sensors that can be deployed to measure PM exposures in pediatric asthma patients. The ideal sensor needs to be able to differentiate between various types of PM. This will allow for the identification of the particle types that aggravate asthma along with being able to distinguish allergens from other particulates in the air. For example, some children's asthma is aggravated by pollen while others are most sensitive to traffic-related PM.⁷⁻⁹ Pollen and traffic emissions have drastically different chemical and physical properties.^{10, 11}

The target sensor needs to be wearable so it goes with the child and measures the actual particulates to which a child is exposed. Throughout the day people are exposed to different microenvironments which have varying particulate matter concentrations due to the different sources that affect the environments differently.^{12,}
¹³ These different environments affect one differently and require a higher temporal and spatial resolution than stationary measurements provide. Often, PM concentrations in different microenvironments have no correlation with the concentrations measured by stationary instruments deployed for ambient regulatory monitoring.^{14, 15} This sensor will help determine the air quality in the various microenvironments which a child is exposed to throughout the day and help determine the environmental factors affecting pediatric asthma on the individual level. Also, most regulatory PM monitoring stations employ 24-h integrated measurements. Asthma, though, is often aggravated by acute exposure to PM on timescales shorter than 24 h.^{6, 16} This means that our ideal sensor needs to provide

measurements with a fast response time to capture episodic peaks in PM concentrations that may occur throughout the day. As a wearable sensor, our sensor will need to be lightweight, small, and have a low power consumption. These factors allow the device to be portable and worn throughout the day.¹⁷⁻²⁰

The work described in this thesis is part of the Pediatric Research using Integrated Sensor Monitoring Systems (PRISMS) Research Grant from the National Institutes of Health (NIH). This grant funds research into the development of a low-cost, low-power, wearable sensor to measure the environmental triggers of asthma.

The following factors were considered during the design of the environmental sensor for the triggers of asthma:

- The sensor must be a wearable, low-cost particulate matter sensor for use in research causes of asthma aggravation.
- The sensor needs to accurately measure particulate matter in the air.
- The sensor shall determine/identify the type of particulate matter, e.g. pollen or smoke, to help to identify allergens and PM sources that lead to asthma aggravation to inform source avoidance.

The research accomplished in this phase of the project was a detailed characterization of the Shinyei PD42NS under its default configuration and with several modifications. The Shinyei PD42NS is a commercial, low-cost (~\$15) PM sensor that uses light-scattering (nephelometry) as the measurement principle. The Shinyei sensor has been used to measure ambient PM concentrations and is one of the most widely used low-cost PM sensors on the market. Numerous studies investigating the Shinyei's effectiveness in both lab and ambient conditions have

been published.²¹⁻²³ The characterization of the Shinyei sensor was done to understand the strengths, weaknesses, and general operation of a current low-cost sensor to inform the design and development of the UMBC prototype sensor.

2.0 Background

2.1 Particulate Matter

Particulate Matter (PM), also known as aerosols, is solid and liquid particles suspended in the air. It is one of the six criteria air pollutants regulated by the Environmental Protection Agency under the Clean Air Act.²⁴ Particulate matter is classified as coarse, where particulates have diameters ranging from 2.5 to 10 μm , and fine ($\text{PM}_{2.5}$) where particulates have diameters less than 2.5 μm . These categories exist due to increased health risks posed by smaller particulates in the $\text{PM}_{2.5}$ category. Particulate matter is classified as either primary or secondary. Primary aerosols are directly released into the atmosphere, while secondary aerosols are formed from gases reacting in the atmosphere.

2.1.1 Sources of Particulate Matter

There are many sources of particulate matter that are both natural and anthropogenic in nature. Common natural sources of particulate matter are volcanoes, mineral dust, and sea spray. A common anthropogenic source is fuel and biomass combustion. Particulate matter is either a primary aerosol (directly released to the atmosphere) or secondary aerosol (particulate formed in the atmosphere). Secondary aerosols include sulfates, nitrates, and organics formed from VOCs.²⁵ Combustion of fossil fuels has been shown to be a major source of particulate matter in cities.²⁶ A major source of particulate matter from fuel combustion is car emissions. Numerous studies have shown elevated particulate concentrations in traffic and near roadways.^{5, 6, 10, 14, 27-30}

2.1.2 Regulatory Standards

The EPA has established the National Ambient Air Quality Standards (NAAQS) which regulate the ambient air quality in the United States. The World Health Organization (WHO) has published standards for ambient air quality limits based on particulate matters' effect on human health. The NAAQS and WHO standards are shown in Table 2.1; the NAAQS standards are the regulatory limits for ambient air quality in the US.

Table 2.1: Particulate Matter Ambient Regulations

Particulate Matter Regulatory Designation			NAAQS ($\mu\text{g}/\text{m}^3$) ³¹	WHO ($\mu\text{g}/\text{m}^3$) ³²
PM _{2.5}	1 year	Primary	12.0	10.0
		Secondary	15.0	
	24 hr	Primary and Secondary	35.0	25.0
PM ₁₀	1 year	Primary and Secondary	150	20.0
	24 hr			50.0

2.1.3 Ambient Particulate Matter Concentrations

There is significant variation in PM concentrations depending on proximity to the source of the PM. In an analysis of US cities, the ambient PM_{2.5} concentration was found to range between 4.14 to 22.7 $\mu\text{g}/\text{m}^3$ with means for different clusters within the cities ranging from 12.2 to 14.1 $\mu\text{g}/\text{m}^3$ based on the age of the city and usage of air conditioning.³³ This shows that ambient PM in the U.S. has concentrations in the range of the NAAQS standards. This implies that a sensor needs to be able to distinguish PM at these low levels.

2.1.4 Particulate Matter size distributions

The distribution of particles in the atmosphere is characterized based upon the number of particles as a function of particle diameter, or based on the volume (or mass) of particulate matter as a function of particle diameter. The number distribution represents the number of particles at each size while the mass distribution represents the mass of particles at each size. The number distribution is based on the count of particles of each size. The mass distribution is based on the mass of particles present at each size. For example, if a system has 10 1 μm particles of uniform composition and 1 10 μm particle of the same composition, then in the number distribution will show the larger number of 1 μm particles whereas the mass distribution will show the greater mass of the 10 μm particle.²⁵

In a typical urban environment, the number distribution tends to show that the majority of particles are less than 0.1 μm while the volume distribution shows two peaks, one between 0.1 μm and 1 μm (the accumulation mode) and the other between 1 μm and 10 μm (the coarse mode). This distribution shows how most particulate matter are fine aerosols and shows the significance of detecting smaller particles. In a study on bioaerosols, which are common allergens for many people, on dry days, it tends to be mostly coarse particulates like pollen, but after a rain event the coarse particulates mostly washout leaving behind only the fine particulates.¹¹

2.1.5 Health Effects of Particulate Matter

Particulate matter has been shown to have many adverse health effects, which include effects from both chronic and acute exposures. Acute effects of particulate matter are death from respiratory and cardiovascular diseases, increase in

hospitalizations, heart attacks, and lung inflammation. Chronic effects of particulate matter are slowed lung growth, the development of asthma, damage to lungs, death from cardiovascular disease, hospitalization from asthma, and low birth weight.^{1, 4, 5, 8, 9, 33-61} Particulate matter is the largest environmental health risk with ambient particulate matter concentrations attributed to 76 million disability-adjusted life years lost and household air pollution from solid fuel combustion attributed to 108 million disability-adjusted life years lost worldwide in 2010.⁴³ Particulate matter has been shown to increase mortality by 0.33% for each increase of 10 $\mu\text{g}/\text{m}^3$ in $\text{PM}_{2.5}$.³³ During the Utah Valley Steel Mill Strike, many health effects of particulate matter were discovered due to a 43% reduction in ambient PM_{10} . There were reductions in hospital admissions for asthma, bronchitis, pleurisy, and pneumonia. The respiratory and cardiovascular mortality also decreased during the period of the shutdown.⁵³ A similar situation occurred during the copper smelter strike of 1967, during which there was a decrease of about 60% of sulfate particulates which correlated with a 2.5% decrease in mortality in Arizona, Nevada, New Mexico, and Utah.⁵² On the other hand, coarse particulate matter has been shown to have a weak correlation between short-term exposure and ambulance dispatches,⁴⁵ while fine particulate matter has a stronger correlation between short-term exposure and ambulance dispatches for respiratory diseases.⁴⁶

2.1.5.1 Asthma

Particulate matter is known to both exacerbate asthma and can lead to the development of asthma. Particulate matter affects developing lungs and can affect the development of asthma in children younger than fourteen. The different types of

particulate matter that affect asthma are dust, dander, mold, and smoke along with elevated levels of ambient air pollution. Asthma patients react differently to these different particulate types with variance in allergies and phenotypes of asthma. In a survey of asthma patients, 72% of participants claim that dust is a trigger for their asthma, 59% smoke, 58% air pollution, 51% mold, and 50% animals.⁹ Particulate matter inflames the lung and can also increase sensitivity to allergens.^{3, 7, 9, 16, 42, 49, 62} Exposure to PM increases hospitalization among children with asthma.^{16, 63} PM from fuel combustion has been found to especially exacerbate asthma^{6, 16} and increase the chance of development of asthma.⁶ There can be up to a 24-h lag between exposure to particulate matter and the exacerbation of asthma.⁹

2.2 Microenvironments

Wearable sensors provide a measure of an individual's exposure to particulate matter encountered in the different environments that they inhabit. Since there can be spatial variation of particulate matter that is not discernable by widespread air quality sensor networks, the use of wearable sensors is critical to measure individual PM exposures. The stationary monitoring sensors are often not representative of the exposure of the average person.^{14, 15, 35, 64-68} People spend about ninety percent of their life indoors,⁶⁹ so it is important to consider the indoor environment in addition to the variations in outdoor PM. Particulate matter in indoor air is often different due to the variation of sources, such as cooking, dust, dander, and indoor smoking.⁷⁰ Personal exposure has been found to be as much as twelve times higher than that estimated from outdoor, stationary measurements.⁶⁵ On biking routes, there has been significant variation in particulate matter measured with concentrations ranging

between 45.5 to 79.8 $\mu\text{g}/\text{m}^3$. The higher concentrations occur near traffic lights and other locations where traffic slows and stops. The concentration was also affected by buildings and wind velocity.¹⁴ Green areas have been shown to have lower concentrations of particulate matter.⁷¹ Homes with larger yards have been shown to have lower indoor and outdoor particulate matter concentrations along with lower overall exposure to the residents.⁷¹ High levels of fungal and bacterial bioaerosols indoors have been found exceeding the acceptable maximum values for personal exposure.⁷²

2.3 Nephelometry

Nephelometry is the measurement of light scattered by particles. Light scattering can be divided into three categories: elastic scattering, quasi-elastic scattering, and inelastic scattering.²⁵ Elastic light scattering occurs through the processes of reflection, refraction, and diffusion where the wavelength of the light does not change. Reflection is when light bounces off the surface of a particle. Diffraction is the process where light is bent around the edge of the particle when passing next to a particle. Refraction is the primary form of scattering by particulate matter and is described below. Inelastic light scattering occurs through processes such as Raman scattering and fluorescence, where the scattered wavelength is different from the incident light.²⁵

Refraction is the change in angle of light's path due to movement through a boundary of two different materials. For example, light entering a particle from the air and then exiting the particle back to air is bent or refracted both going in and leaving the particle. The amount of refraction of the light is dependent on the type of

particle. The ratio between the refractive indexes of the two materials determines how much the light will be bent or changed when crossing a boundary. The refractive index for a vacuum is 1 and is essentially 1 for air.²⁵ Different materials have different refractive indexes and cause different amounts of light refraction.

The complex refractive index equation is shown below, with n being the real value and k being the imaginary value. The imaginary component relates to the amount of light that is absorbed by a particle.

$$N = n + ik$$

Below is a Table 2.2 of refractive indexes from different sources.⁷³⁻⁷⁹

Table 2.2: Sample Refractive Indexes

Location/Type	Refractive index	
	n	k
Average ambient aerosol	1.5	0
Average dry aerosol	1.57	0
Ambient aerosol	1.53	0.02
Inorganic nitrates and sulfates	1.53	0
Organic aerosols	1.5-1.55	0
Saharan mineral dust	1.5-1.55	0
Secondary organic aerosols	1.45-1.7	0.0 – 0.04
Large dust particles	1.5-1.6	0
Urban Aerosols	1.37-1.6	0
Mixed Industrial Aerosol	1.35-1.45	0.0 – 0.01
Biomass Burning	1.425-1.55	0

2.3.1 Mie Theory

Mie Theory describes the magnitude of light scattering caused by a single particle. Mie Theory is a derivation of the Maxwell Equations, which describe how electromagnetic waves travel through space. Mie theory solves for the scattering of light from a homogeneous spheroid using the Maxwell Equations. Light scattering is dependent on particle diameter, wavelength, and the refractive index of the particle composition. Mie theory can be used to explain how multiple particles scatter light. Therefore, the scatter from a group of particles can be scaled from the scattering of a single particle.²⁵

2.3.1.1 MiePlot 4600

The MiePlot 4600 (<http://www.philiplaven.com/mieplot.htm>) is a software application which simulates Mie scattering. It allows for variation of the independent variables which affect scattering intensity and calculates the scattering intensity based on the system of equations presented by Bohren and Huffman.⁸⁰ Scattering intensity

is dependent on refractive index, particle size, wavelength, and scattering angle. The refractive indices of atmospheric particles in urban environments have been found to range between 1.5 to 1.6 with the imaginary component ranging from 0 to 0.005.⁷³

2.3.1.2 Ångström exponent

The Ångström exponent correlates the relationship between wavelength and scattering coefficient. The Ångström exponent is used to determine the size of particles being measured. The equation below shows this relationship:

$$\frac{\sigma_{\lambda}}{\sigma_{\lambda_0}} = \left(\frac{\lambda}{\lambda_0}\right)^{-\alpha}$$

where σ_{λ} is the scattering coefficient, σ_{λ_0} is the reference scattering coefficient, λ_0 is the reference wavelength and λ is the wavelength. α is the Ångström exponent.

The Ångström exponent is related to the particle size distribution. Lower Ångström exponents indicate a greater contribution from large particles. The Ångström exponent varies from 0.25 to 3.2 in urban environments.⁷³ The Ångström exponent had an average value of 1.4-1.7 over India.⁸¹ There is seasonal variation with higher values of the Ångström exponent in the winter and lower values in the summer. This is due to biomass burning and fuel consumption in the winter which release lots of fine particles into the atmosphere.⁸² A critical element of the Ångström exponent is its size dependence: fine particles typically have values between 1.5 and 2, while coarse particles having values that approach zero.^{81 83}

2.4 Low-Cost Sensors

Dense monitoring networks are made economically viable using low-cost sensors with numerous sensors deployed over a relatively small geographic region. The sensor network provides greater coverage in determining spatial variation in particulate matter concentrations.⁸⁴ There are often hotspots, such as roadways and industrial centers, which can be identified through network measurements. Without a network of sensors, it would be far more challenging to identify local sources and work to address them.¹³

The strength of low-cost sensors is their ability to be deployed in much denser networks to give greater spatial and temporal coverage.⁸⁵⁻⁸⁷ The low-cost sensors can be used in a wearable platform to provide an individual measurement of particulate matter exposure. Some low-cost sensors take real time measurements instead of having a day-long integrated concentration like filter-based measurements employ, providing much better temporal information. Low-cost sensor networks offer the potential to significantly improve the spatial understanding of PM sources.¹³ The weakness of low-cost sensors is their lack of accuracy and precision.⁸⁸ Low-cost PM sensors also have a variation in response based on the particles measured, which is problematic given the diversity of aerosol composition found in different locations.

A variety of low-cost particulate matter sensors were tested with cigarette smoke and Arizona road dust.⁸⁸ Several of these were found to be very accurate. The Speck is a sensor setup using Syhitech DSM501A sensor. The TSI AirAssure and UB AirSense use the Sharp GP2Y1010AU0F sensor. The regression fits are

shown in the Table 2.3 where the sensors were compared to values measured by an aerodynamic particle sizer from TSI.⁸⁸

Table 2.3: Regression Closeness of Fit for various PM Sensors

Sensor	Cigarette Smoke R ²	Arizona Road Dust R ²	Cost (\$)
Speck 1	.92	.96	200
Speck 2	.92	.96	
Dylos 1100 Pro	.67	.89	200
Dylos 1700	.7	.85	425
AirAssure 1	.45	.98	1,500
AirAssure 2	.99	.94	
AirAssure 3	.42	.98	
UB AirSense	.85		100
Grimm	.89	.98	25,000

Other studies have shown that low-cost PM sensors have highly variable results, where there are both strong correlations (R² values 9) and weak correlations (R² values between 0.4-0.6) that depend on concentration and PM type. Studies show the promise of using the low-cost sensors, but there is a strong need for the improvement in accuracy and precision.^{21-23, 84-97} The low-cost sensors have the limitation in that they are not able to be calibrated to an EPA reference instrument yet, because there is too much variability in response to varying particulate types. Thus, the calibration can vary significantly from location-to-location, and even instrument to instrument. Alternately, the calibration can change in a fixed location with changes in the aerosol composition. If the sensor is calibrated in one location, that does not mean it is well calibrated for a different location.²² For example, low-cost sensors have been shown to work better in areas with lower traffic than in areas with higher traffic. In areas with high traffic, the PM was just released to the atmosphere. In areas with low traffic, the PM has changed by aging and

restructuring. The low-cost sensor was better able to identify the older PM. The sensors have been shown though to provide a qualitative indication of the air quality; for example, whether the conditions are good, moderate, or poor.⁸⁵

2.4.1 Shinyei

The Shinyei PPD42NS sensor is a particulate matter sensor which uses the principles of light scattering. It detects the amount of light scattered by the sampled PM. The Shinyei sensor has been tested with ambient concentrations along with lab testing of a variety of particulate types and sizes. The strength of the Shinyei is its low cost (\$15), its ease of operation, along with the other advantages listed above.^{21, 23, 98} The weakness of the Shinyei sensor is the lack of accuracy and precision, similar to limitations encountered with other low-cost sensors.^{21, 23, 98} The Shinyei sensor is sensitive to the orientation due to the instrument design, which uses convective flow produced by a resistor as the method to sample air into the sensor. The Shinyei sensor also has a variation in response based on the type of particles measured. The Shinyei sensor shows accurate calibrations with specified particulate types and sizes.^{21, 23} When the Shinyei sensor measures ambient PM concentrations, the goodness of fit decreased compared to measurements in the lab with a single aerosol type, likely due to the variation in ambient particulates.^{22, 86}

The Shinyei sensor has been shown to have a high dependence on composition and size of the particles, with a higher response observed for larger particles as compared to smaller particles.^{23, 21} The Shinyei sensor had a limit of detection of $1 \mu\text{g}/\text{m}^3$ for PSL.²¹ The Shinyei sensor has been found to have a limit of detection of $6.44 \mu\text{g}/\text{m}^3$ in one study and $9.1 \mu\text{g}/\text{m}^3$ by another for incense smoke

(this difference was noted and unexplained in Bergin et al.) and an R^2 value of 0.93 when compared to the TSI DustTrak sensor.²³ The Shinyei was found to have a variance in R^2 values of between 0.66 to 0.99 depending on the particulate type measured when compared to measurements from a TSI aerosol particle sizer.²¹ Another study observed much lower R^2 values (0.20) when compared to measurements from a TSI DustTrak sensor; however, this study was conducted using particles from incense smoke.⁹⁸ The lower R^2 value observed for the test with incense smoke was likely due to variations in signal processing and sampling time. The Shinyei sensor has a high dependence on the relative humidity, but temperature does not appear to have a large effect on the accuracy of the Shinyei sensor.^{21, 23} During testing in California, the Shinyei sensor was evaluated for the measurement of ambient concentrations of PM. The study determined there was a correlation of the Shinyei to the DustTrak monitor (see Section 3.4.2), with R^2 values between 0.64-.7 for the period of the measurements.²² The Shinyei demonstrated a much stronger correlation to the DustTrak during tests in China, where R^2 values of 0.85-0.97 were obtained.⁸⁶ Our work builds upon these prior studies by further characterizing the base (i.e., commercial) Shinyei sensor, and by characterizing the sensor with a number of modifications.

3.0 Methods

3.1 Shinyei PD42NS

The Shinyei PD42NS sensor detects and measures airborne particulate matter by measuring the intensity of the light scattered by the particles in the air sample. The level of the scattered light is proportional to the concentration of the particulate matter for a given particulate type and size. The Shinyei uses a resistor to heat air which creates airflow into the sampling chamber. The resistor heats the air at the bottom of the sampling chamber and the air rises due to the temperature difference between the top and the bottom of the chamber using convective airflow. This method of creating airflow, therefore, requires the Shinyei sensor to be kept in an upright configuration.

The Shinyei PD42NS illuminates an infrared LED at 839 nm through a collimator and a focusing lens to focus the light at the sampling stream as it passes through the sampling chamber. Some of this light is scattered by the particulate matter in the air, and the photodiode detects the light scattered by the PM in the sampled air. The photodiode produces an output voltage related to the amount of scattered light that it receives. The Shinyei has two outputs: for the first output, the P1 comparator is set to be triggered when the voltage from the photodiode is greater than 1 V. For the second output pin, the P2 comparator is set to be triggered when the voltage from the photodiode is greater than 2.5 V. This can be lowered using the threshold pin. Setting a threshold is meant to reduce instrument noise or boost the signal from the photodiode. In theory, the higher the threshold is set, the less noise there will be, and the lower the threshold is set, the greater the signal will be. The

comparator outputs either a high or a low voltage; the default output when the photodiode signal is below the threshold is the high voltage state, but when the comparator is triggered (i.e., when particles are detected) it outputs a low voltage. The concentration of the particulate matter can be determined from the percentage of the sampling time where the voltage is low (detecting particles). This low voltage occupancy corresponds to the concentration of particulate matter.

3.2 Shinyei PD42NS UMBC Prototypes

In researching improvements on the Shinyei sensor, four different prototypes were designed and built. These prototypes were designed to test for various improvements to the Shinyei sensor. These are briefly described in Table 3.1, with more details in the descriptions following the table.

Table 3.1: Prototype Modifications

Prototype	Fundamental Modification
Prototype-R	A potentiometer is placed between the threshold pin and ground to modify the threshold voltage of P2 by adjusting the resistance
Prototype-F	A fan is added to the sensor to increase sample flow.
Prototype-P	A piezo pump is added to the sensor to increase flow through the sensor and allow for variable flow control.
Prototype-G	The infrared LED in the Shinyei is replaced with a green (530 nm) LED

Prototype-R was a base Shinyei Sensor with a potentiometer between the threshold pin and the ground pin. The potentiometer allows for the resistance

between the threshold and the ground to be adjusted, which changes the threshold for the output pin, P2. With a lower threshold, the sensor is triggered with less light being scattered. In theory, the potentiometer allows for smaller particles and lower concentrations of particles to be detected. It may also increase instrument noise, especially at low aerosol levels. This was evaluated through a series of experiments.

The second prototype, Prototype-F, is a base Shinyei sensor with a fan added in place of the heated resistor. This fan increases the air flow rate of the sensor. An increased flowrate ensures a homogenous concentration between the sensor chamber and the external air. This increased flowrate helps prevent artifacts from the environment such as wind. Also, having a fan or a pump actively sample the air instead of the convective-based flow should allow for changes in sensor orientation. This means that the sensor should function consistently under changing orientations, such as would occur in a wearable platform and deployment.

The third prototype, Prototype-P, is a base Shinyei sensor with a piezo pump used to control the sample flowrate of the sensor. Piezo pumps are designed to create low flows of liquids and gases. The piezo pump's flow rate can be varied based on the voltage supplied to the pump. The pump creates a larger pressure drop than the fan and the resistor allowing for higher air flow rates to be delivered to the sensor.

The Figure 3.1 shows the relationship between the voltage provided to the pump and the air flowrate, which was measured using a bubble flowmeter. The pump was attached to the flowmeter in either a pushing or pulling configuration. Figure 3.1 shows that the pump's flow rate was linear with the voltage over the range of 17 – 30 V. It also shows a consistent flow rate was achieved in either the pushing or pulling

configuration. This indicates that the piezo pump offers excellent flexibility in its potential use with a wearable sensor. This is important since this shows the ability to tightly control the flowrate using the piezo pump.

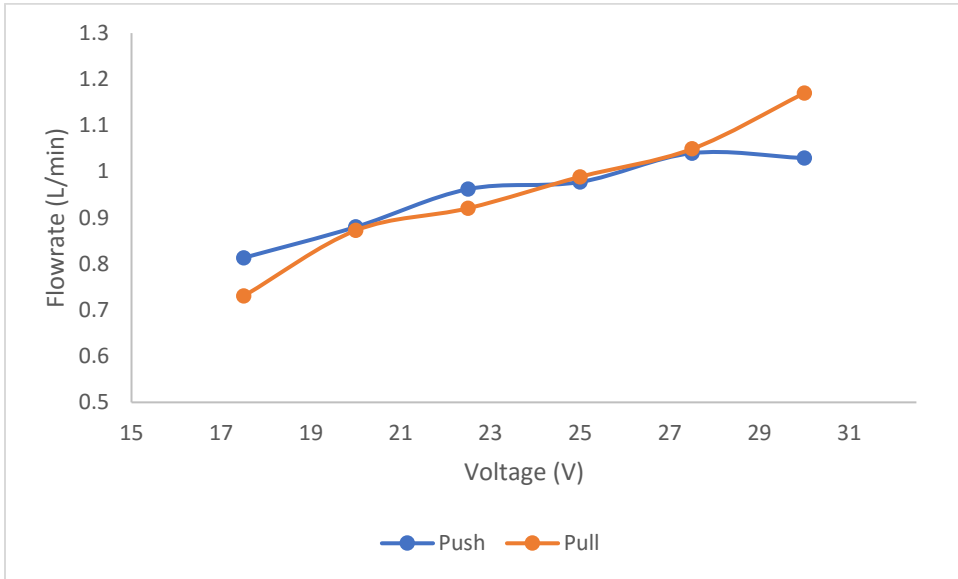


Figure 3.1: Piezo pump flow calibration as a function of input voltage.

A green LED was installed in place of the infrared LED in Prototype-G to test the performance of the Shinyei PD42NS using a different wavelength than the standard Shinyei PD42NS. According to Mie theory, the intensity of light scattered varies with wavelength.²⁵ The change in wavelength is used to investigate how the light scattering by different particulate types varies in relation to wavelength.

3.3 Particulate types

Three different types of particulate matter were used in the experiments, chosen to cover a broad range of atmospherically relevant conditions. These include NaCl, PSL, and incense smoke. These different particulates were also varied over size as well as type.

NaCl is a common inorganic aerosol originating from sea spray and road salt. NaCl is also a commonly used reference aerosol with similar properties to other inorganic aerosols such as ammonium sulfate.²⁵ In this research, NaCl concentrations between 0.5-0.01 M (aqueous concentration basis) were used for particulate generation. Figure 3.2 shows the relationship between particle size and aqueous concentration as measured and recorded by TSI.⁹⁹

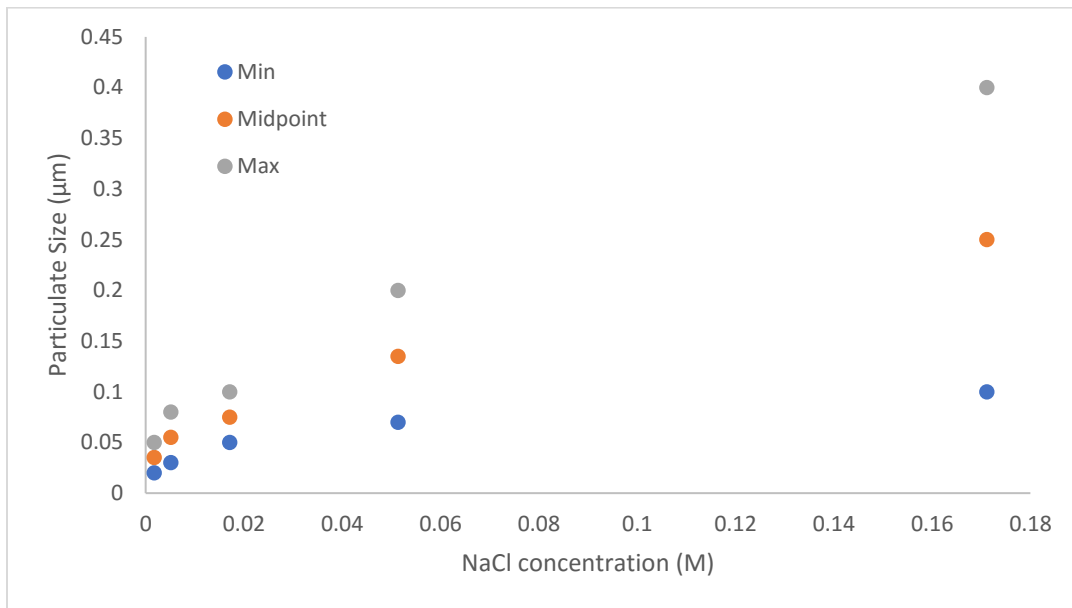


Figure 3.2: Relationship between aqueous NaCl concentration and particle size generated by the atomizer.

PSL are standardized sized particles designed as reference aerosols with uniform sizes for use in lab testing. In this research, 0.5 µm, 1 µm, and 2 µm diameter PSL were used. These particles allow for the variance in response in relation to the size of the particle using standard sized particles.

Incense smoke was also used as a particle source, since combustion is such a prevalent source of particulate matter in both indoor and outdoor environments. Incense is a smoke source which creates high PM concentrations. Incense is

commonly burned indoors and can be a significant contributor to indoor exposures when it is used.^{70, 100} The PM generated from incense combustion can have similar physical and chemical properties to other common sources of smoke, including wood burning and cigarette smoke.¹⁰¹

3.4 Experimental Set-up

The experimental set-up was different when incense was used as the particulate matter source compared to when NaCl or PSL was used. For an incense run, the incense was held in a candle holder filled with sand placed in the sampling box (Figure 3.3). The Shinyei sensors were oriented vertically and a fan was employed to ensure complete mixing within the air sampling box. The DustTrak was located outside of the sampling box and continuously pulled a sample out of the box through the conductive tubing.

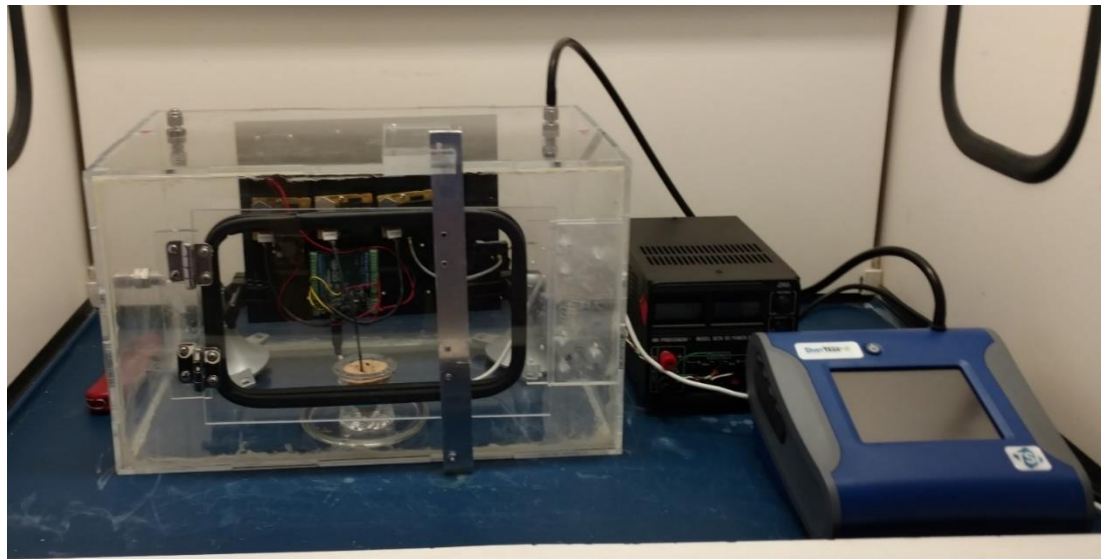


Figure 3.3: Experimental setup for an incense test.

For the NaCl and the PSL runs, the experimental setup was similar to the incense test in all regards, except the PM generation procedure. For PM generation,

the appropriate aqueous solution was placed in the atomizer. The compressor creates a flow of filtered air into the atomizer where droplets of the aqueous solution are produced. The droplets then enter a dryer where the water is removed and solid particles are formed. Crystallization happens between 46-48% relative humidity for NaCl.¹⁰² The relative humidity in the sample box was measured to be between 20-23% during runs using the Omega temperature and relative humidity sensor. The particles then enter the sampling box. This setup is shown in Figure 3.4.

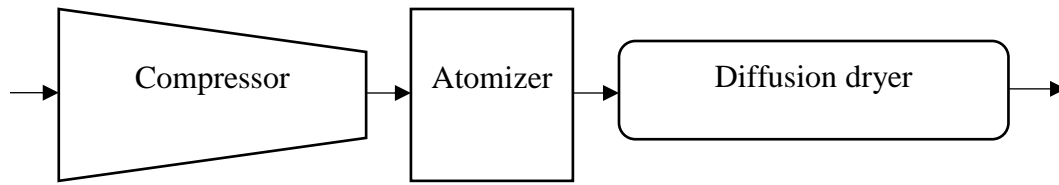


Figure 3.4: Schematic showing PM generation for NaCl and PSL tests.

The sampling box is two cubic feet with an inlet for particulate matter to enter, an outlet for the DustTrak to sample, and an outlet for the wires to power the sensors inside the sampling box. The sampling box was coated with anti-static spray to reduce the rate at which particles are lost to the walls. This box allows a high concentration of particulate matter to be contained safely for testing of the different prototype sensors. The air inside of the box is circulated by a fan in the box creating a homogenous mixture so that all the sensors have the same concentration of particulate matter and can, therefore, be directly compared to each other.

The TSI Model 9302 atomizer is an aerosol generator. The atomizer can suspend various particulates in a liquid solution into the air, such as NaCl and PSL. The atomizer operates by having a liquid of a known solution in the atomizer. The atomizer has an adjustable flow based on the pressure setting for the compressed air. When in use, the atomizer had a pressure between 20 to 25 psi, which produces an output air flow of between 5.7 to 6.6 L/min. Compressed air is then pumped into the atomizer to form a jet stream of the liquid droplets leaving the atomizer propelling the solution into the air. The output of the atomizer is connected to the diffusion dryer described below.

The diffusion dryer is a 0.6 m long tube of silica gel that absorbs the water from the droplets leaving the atomizer. The silica gel is held to the sides of the tube

with a fine metal mesh. The silica gel removes the water as the air flows down the dryer. In this tube, the removal of the water ensures the refractive index of the solid particles is consistent. This is important to ensure that the sample particulates are solid particles, not aqueous droplets.

During the testing of the Shinyei sensor, dynamic blanks of the system were regularly run. These blanks mimicked a normal PSL or NaCl run, except with ultrapure DI water in the atomizer instead of a PSL or NaCl solution. These blanks were used to show that there was no contamination to the system from previous solutions or from the water in the atomizer. These runs also help to show that the water was effectively removed in the diffusion dryer. An example of a dynamic blank time series is shown in Figure 3.5.

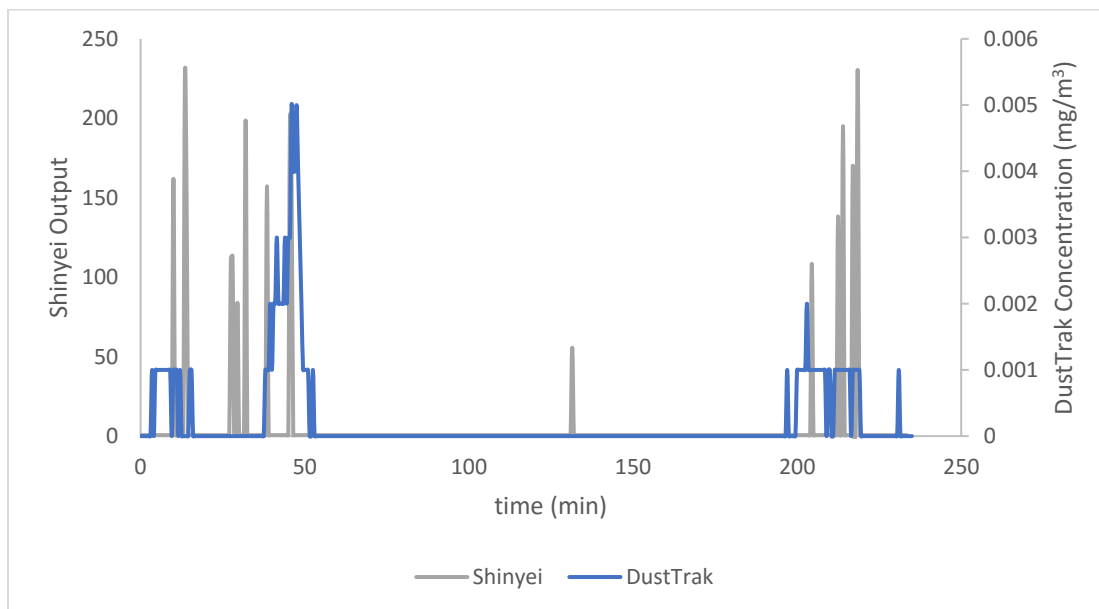


Figure 3.5: Dynamic blank time series experiment

This dynamic blank started with an hour without any water pumped in (background air in the PM chamber only) followed by constant atomizer output (using only pure water) into the system for about 2 hours. Figure 3.5 shows that there

is no correlation between when the water was being introduced through the atomizer and diffusion dryer and the PM concentrations detected by the DustTrak. These readings come from noise within the system, not from residual water. Table 3.2 shows the average readings and the standard deviation for varying series of dynamic blanks, including the test shown in Figure 3.5. Together, Figure 3.5 and Table 3.2 indicate that there was no experiment-to-experiment carryover, and that there were not any fugitive or contamination particles introduced by any of system components.

Table 3.2: Average readings and standard deviation of dynamic blanks

Date of dynamic blank	DustTrak (mg/m ³)		Shinyei	
	Average	Standard Deviation	Average	Standard Deviation
8/11/16	0.0028	0.00066	13.85	48.02
8/12/16	0.0027	0.00064	12.71	44.31
8/17/16	0.00064	0.00128	25.51	53.53
8/30/16	0.000253	0.000676	6.00	29.38

3.4.1 Shinyei Sensor Unit/ Arduino Microcontroller test device

The Shinyei PD42NS Sensor is connected to an Arduino Uno Microcontroller. The Shinyei has two outputs, P1 and P2, which are digital outputs placed into the digital ports on the Arduino. The Arduino is controlled from a laptop and processed the data displayed in the serial logger. The Shinyei sensor's sampling time interval is thirty seconds and the ratio of low to high voltage (low pulse occupancy) is measured. The time that the signal is low is divided by 30 seconds (the sampling time) to determine the low occupancy time percentage.

3.4.2 DustTrak II Aerosol Monitor

The DustTrak II model 8350 Aerosol Monitor (TSI, Inc.) is a commercially available instrument which measures airborne particulate matter. The DustTrak uses the same basic technique, nephelometry, to measure particulate matter as the Shinyei sensor. The DustTrak measures particles between 0.1 μm and 10 μm in size and particulate matter mass concentrations between 0.001 to 400 mg/m^3 with a resolution of $\pm 0.1\%$. The DustTrak also collects particles on a 37-mm filter for off line gravimetric or chemical analysis. The DustTrak was used as the standard measurement against which the various prototypes were compared. The DustTrak II Aerosol Monitor has been used in numerous studies of indoor and outdoor air pollution,¹⁰³⁻¹⁰⁷ and in testing varying low-cost nephelometers for measurement of PM.^{21, 23, 91, 103-110}

3.5 Experimental Test Series

Table 3.3 shows the experimental matrix, with the various particles types shown in the rows and the various prototypes shown in the columns. The number represents the number of duplicate experiments run under each condition, while X's indicate that there were not experiments run in this configuration.

Table 3.3: Experimental Test Matrix

Particle type	Unmodified Shinyei	Prototype-G	Prototype-R	Prototype-F	Prototype-P
Incense	6	2	X	X	X
2 μm PSL	2	X	X	2	2
1 μm PSL	2	2	4	X	X
0.5 μm PSL	2	2	4	X	2
0.5 M NaCl	2	X	X	2	2
0.25 M NaCl	2	1	X	X	X
0.1 M NaCl	1	1	X	X	X

0.05 M NaCl	2	X	X	X	X
0.025 M NaCl	2	1	X	X	X
0.015 M NaCl	1	1	X	X	X
0.01 M NaCl	2	X	X	X	X
0.005 M NaCl	1	X	X	X	X

4.0 Results and Discussion

4.1 Shinyei PD42NS Characterization

The first set of tests was performed to build our basic understanding of the Shinyei sensor in its unmodified state. A series of experiments, listed in Table 3.3, was run with two unmodified Shinyei PD42NS sensors simultaneously with the DustTrak. These Shinyei sensors were run concurrently to determine the consistency of measurements between individual Shinyei sensors. Calibration curves of the outputs of both Shinyei sensors with different particle types (incense smoke, NaCl, and PSL) were created using known particulate matter concentrations between 0 to 5,000 $\mu\text{g}/\text{m}^3$. An example time series of a NaCl run with PM pulsed into the sampling chamber is shown in Figure 4.1. A 2.5-minute rolling average was used to smooth the data collected.

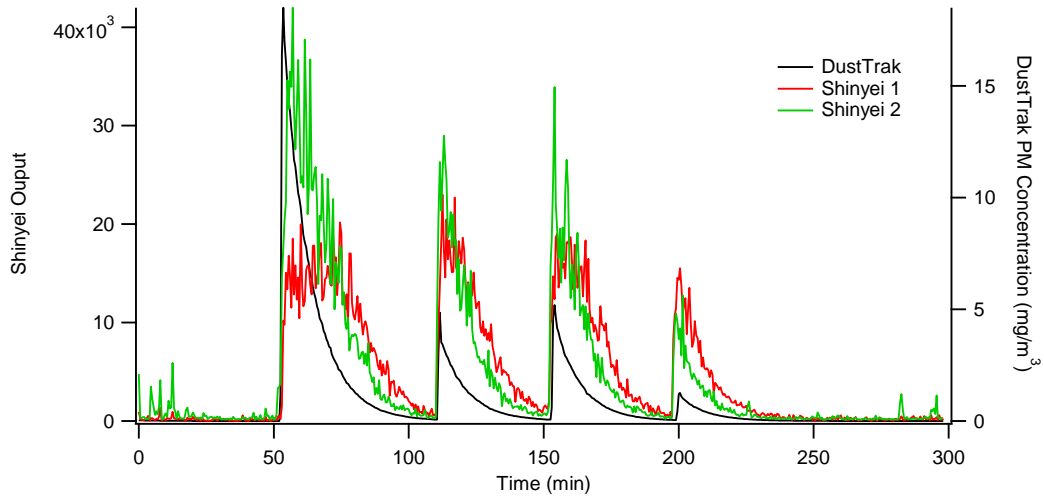


Figure 4.1: Unmodified Shinyei PD42NS & DustTrak II Time Series for experiment with 0.25 M NaCl

The calibration graph between the DustTrak and one of the Shinyei prototypes is shown in Figure 4.2. The DustTrak is a commercially available PM sensor, therefore its output was considered accurate and was used to calibrate the Shinyei prototype sensors. This is consistent with prior studies that use the DustTrak to calibrate the Shinyei and other low-cost sensors.^{91, 103-110}

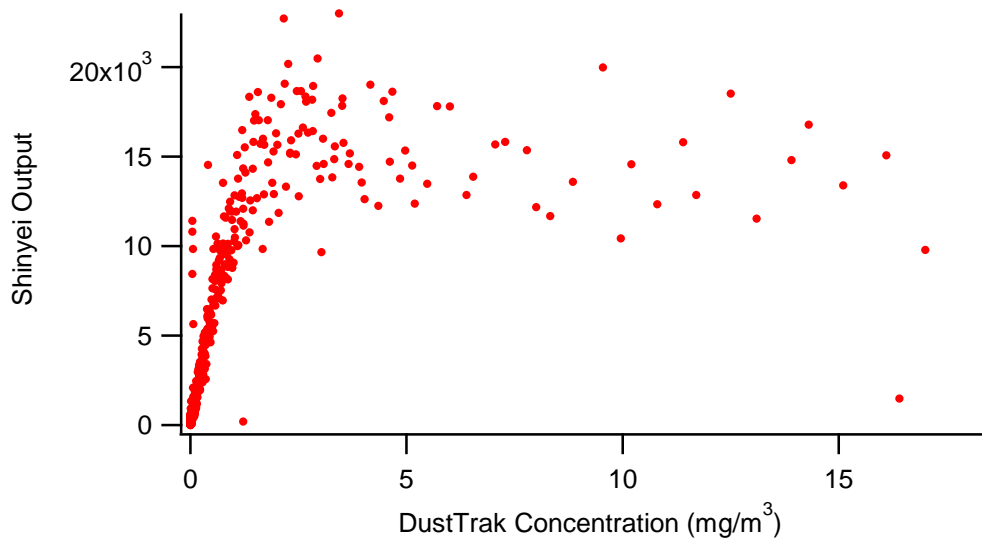


Figure 4.2: Shinyei calibration – 0.25 M NaCl

The data in Figure 4.2 shows that at higher concentrations of particulate matter, the Shinyei sensor unit loses accuracy as the sensor approaches saturation. This has been observed previously, as well.²³ This trend is shown in other test runs with high PM concentrations. However, these concentrations are significantly above typical ambient concentrations and thus highly unlikely to be encountered in normal daily life.³³ Therefore, for the calibration slope, the higher concentrations are not considered in the determination of the calibration curve to enable an evaluation of the sensor performance under more typical ambient PM levels (Figure 4.3).²³

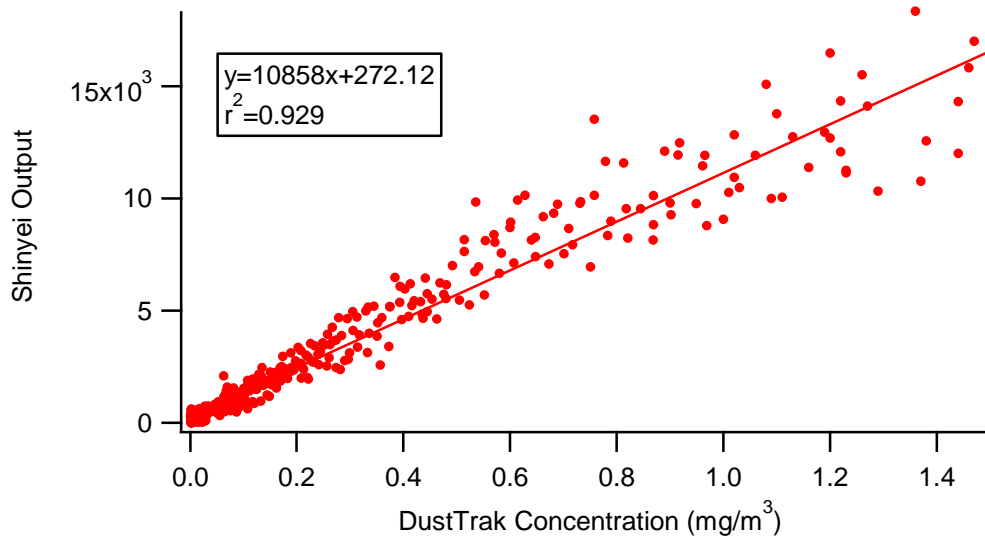


Figure 4.3: Shinyei PD42NS calibration non-saturated region – 0.25 M NaCl

The calibration series for different NaCl concentrations in the atomizer is shown in Figure 4.4. The size of the NaCl PM entering the sampling chamber is directly related to the aqueous NaCl concentration in the atomizer, with higher concentrations producing larger particles. For example, when the concentration is 0.03 M NaCl, the particle size is approximately 0.1 μm , and when the concentration is 0.17 M NaCl, the particle size is approximately 0.25 μm .⁹⁹

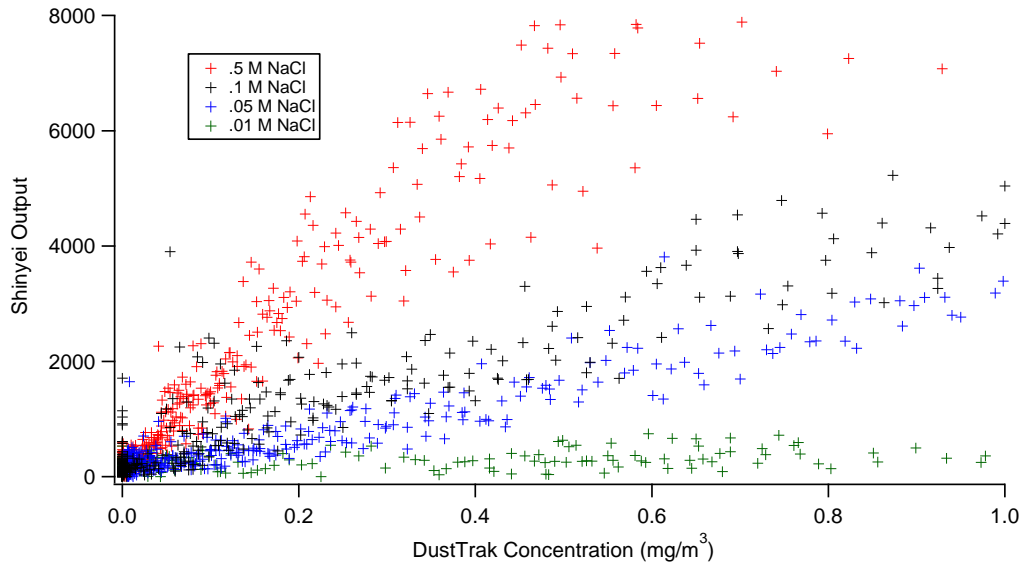


Figure 4.4: Shinyei PD42NS calibration series – NaCl (one point from the 0.5 M NaCl series is off the graph)

The data in Figure 4.4 shows the variance of the sensor unit response in comparison to the NaCl concentration and particle size. The higher aqueous concentrations produce a greater response than the lower aqueous concentrations, strongly supporting the finding that the Shinyei response is greater for larger particles than for smaller particles observed in other studies.^{21, 23} These responses are compared with the other Shinyei responses in Figure 4.8.

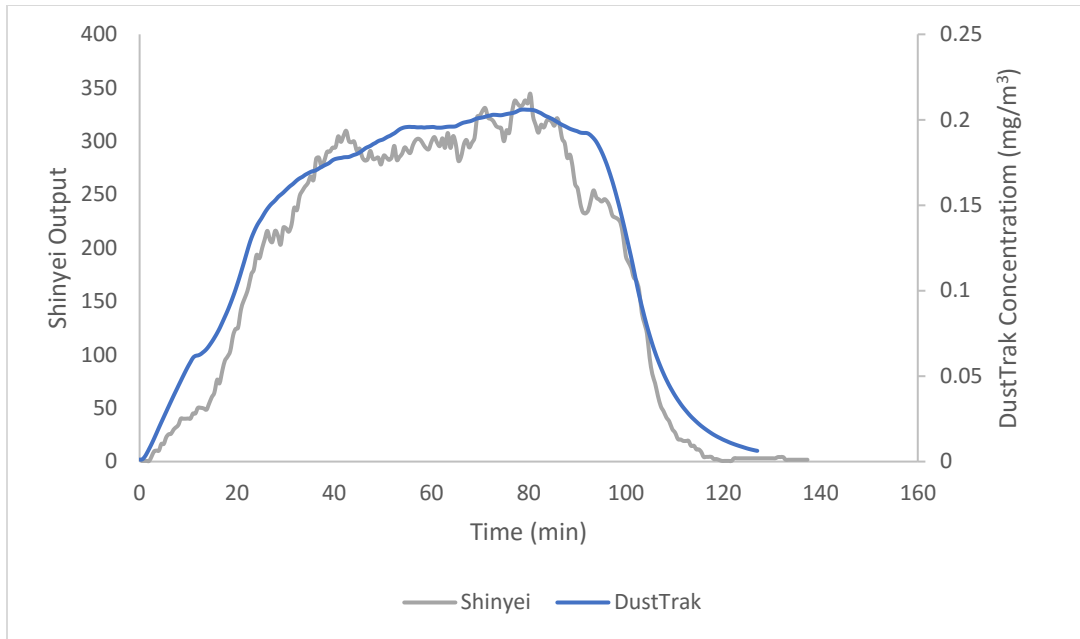


Figure 4.5: Unmodified Shinyei PD42NS & DustTrak II Time Series for experiment with 2 μm PSL

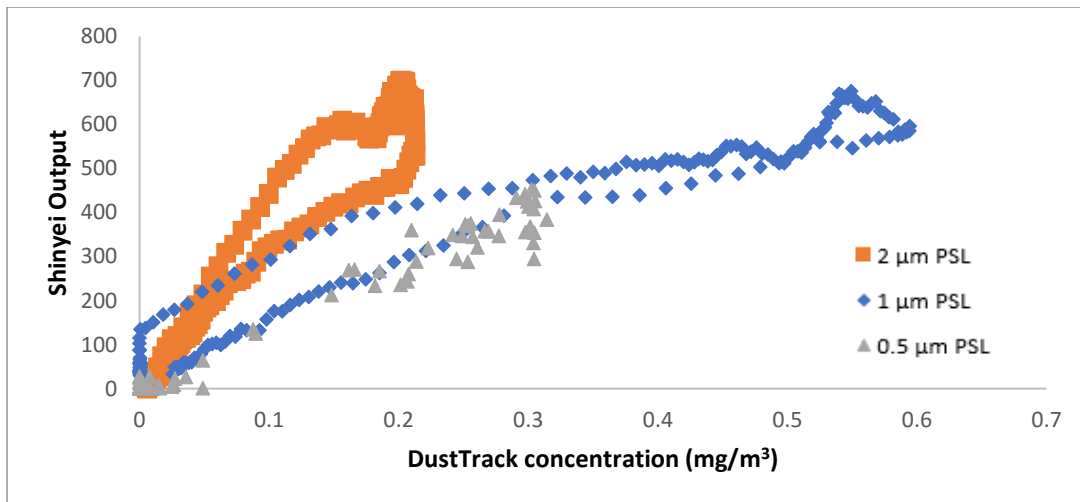


Figure 4.6: Shinyei PD42NS calibration series – Polystyrene Latex microspheres

An example calibration series for the test runs with PSL of 2 μm , 1 μm , and 0.5 μm sizes are shown in Figure 4.6. The two distinct regions of the 2 μm and 1 μm PSL calibrations are caused by variations in the readings when the particulate concentration is increasing and when it is decreasing as seen in Figure 4.5. This may be a function of the experimental setup, and will need to be explored in future studies.

The PSL calibration shows the variance of the Shinyei response as a function of particle size; it has less noise than the NaCl tests. This difference could be due to the uniformity of the PSL in comparison to the NaCl, since the NaCl particle size is correlated to the aqueous concentration but the particles do not have a uniform size (Figure 3.2).

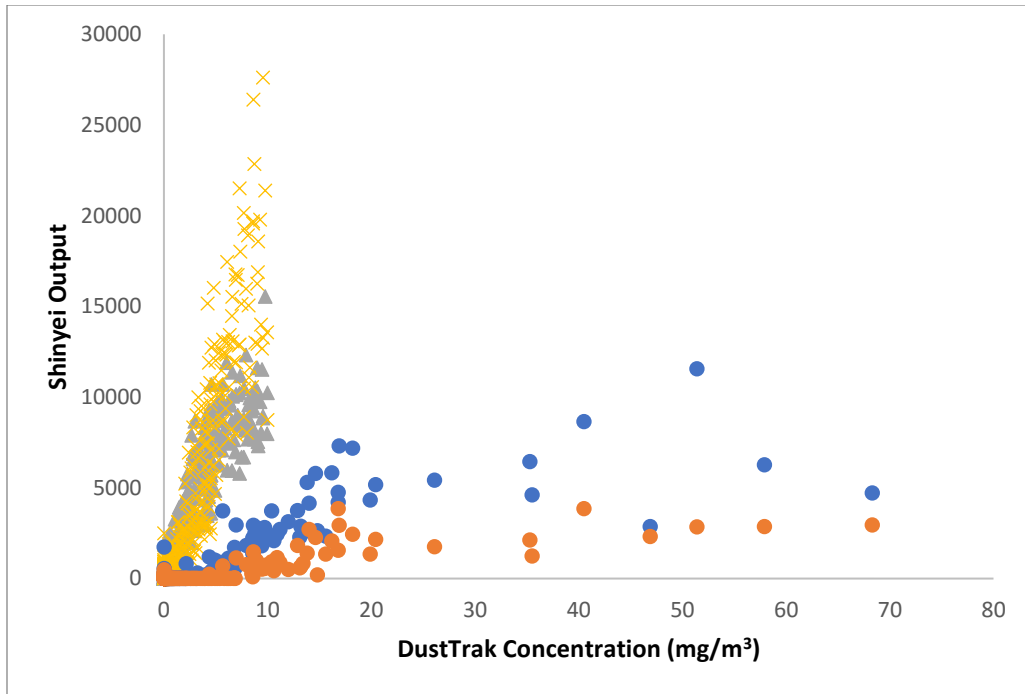


Figure 4.7: Shinyei PD42NS calibration series – Incense

In Figure 4.7, the great variation of slopes for incense runs is shown. This variation is largely due to uncertainty in the size of the particles generated from the smoke. This may help to explain the low R^2 values observed by Bergin et al.⁹⁸ for similar experimental conditions. With these experiments, each individual run had high R^2 values; however, there was significant variability in slopes between each run. This is likely due to variability in the smoke emissions from test-to-test,¹¹¹ since the Shinyeis measuring the same run have similar responses (as seen in Figure 4.7 with the yellow and grey data series being from the same test and the orange and blue data

series being from the other test). The Shinyei showed better repeatability with the NaCl and PSL tests. The slopes of the calibration curves in relation to the particle type and size are shown in Figure 4.8 .

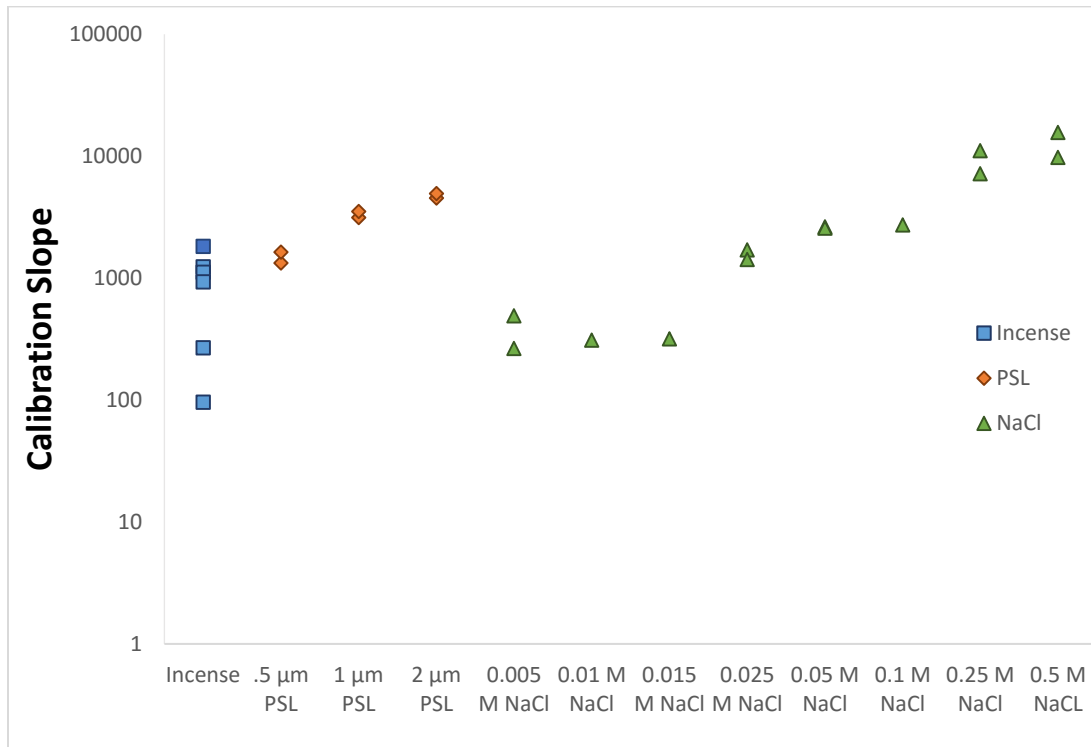


Figure 4.8: Shinyei PD42NS vs. DustTrak slope

In Figure 4.8, the slope for the PSL increases with size in clear and consistent fashion. This was repeatable for each PSL size, as indicated by the multiple tests performed for each size. On the other hand, the NaCl slopes did not follow the same consistent increase with concentration, but showed a less predictable increase with concentration. The aqueous concentration of NaCl is correlated to the size of the particles, but at the lower aqueous concentrations investigated, there was little change in the slope. The atomizer generates a distribution of particle sizes, so this could be due to the percentage of particles which are not detected by the Shinyei. At lower

aqueous NaCl concentrations, few of the particles are detected by the Shinyei, since very little light is scattered and detected by the photodiode. At higher aqueous concentrations (i.e., larger NaCl particle sizes), most of the particles are detected by the Shinyei since the larger particles scatter enough light to trigger the photodetector. Based on our results, it appears that the smallest particle size the Shinyei can detect is $\sim 0.05 \mu\text{m}$ diameter particles, since $0.05 \mu\text{m}$ is the largest particle size produced at the lowest NaCl concentration where there was a response. Note, however, that Figures 4.4 and 4.8 show a very insensitive response of the Shinyei sensors to particles of this size. It is therefore doubtful that the Shinyei would reliably detect particles of this size under ambient conditions if the particle concentrations were orders of magnitude lower.

The variation in the incense runs was far greater than the variation in the NaCl and PSL runs. The incense runs were all characterized by a large variation in the PM emission rate. At times, the incense sticks produced heavy smoke while at other times, the visible smoke was less intense. We hypothesize that the size of the emitted particles varied as well. This would produce the highly variable responses shown in Figures 4.7 and 4.8. The PSL provides a consistent size, and produced good repeatability between tests. The NaCl was also generally repeatable.

The response of the Shinyei PD42NS is dependent on the particle size and type, in addition to concentration. The sensor has a higher response to larger particles over small particles for the same mass concentration. There were approximately two orders of magnitude difference in the response of the Shinyei for the largest and smallest NaCl particles. Further, the sensor had a higher response to NaCl (refractive

index – 1.544) than PSL (refractive index – 1.592) for the same size and concentration.²⁵ With the lower refractive index, more light is detected and provides a greater response: a similar finding was reported by Wang et al.²³ This means that to measure the PM mass concentration with the Shinyei, one must know the particulate type and size. Our results suggest that the Shinyei sensor has limited application as a stand-alone sensor due to the need to know the physical characteristics of the particles being measured. This leads to questions of the accuracy across multiple environments where the particle type and size can vary considerably.

Other studies have shown the variation in response of the Shinyei with size and type of PM, which is consistent with our results. Large particles have higher response, as shown in Wang et al. and Austin et al.^{21, 23} In Wang et al., the variation in particulate type is shown where NaCl, sucrose, and NH₄NO₃ were compared, with NaCl having the lowest response out of the three particle types.²³ The authors suggest that this effect was based on differences in the refractive indices of the particles. Figure 4.8 shows the variation in response in relation to particulate size as shown with the PSL and with the NaCl. Figure 4.8 also shows variation in the Shinyei calibration response with particle size, consistent with the observations of Wang et al. and Austin et al..^{21, 23} This variation in response to particle type and size helps to explain the weaker correlations of ambient measurements compared to laboratory measurements.⁹⁸

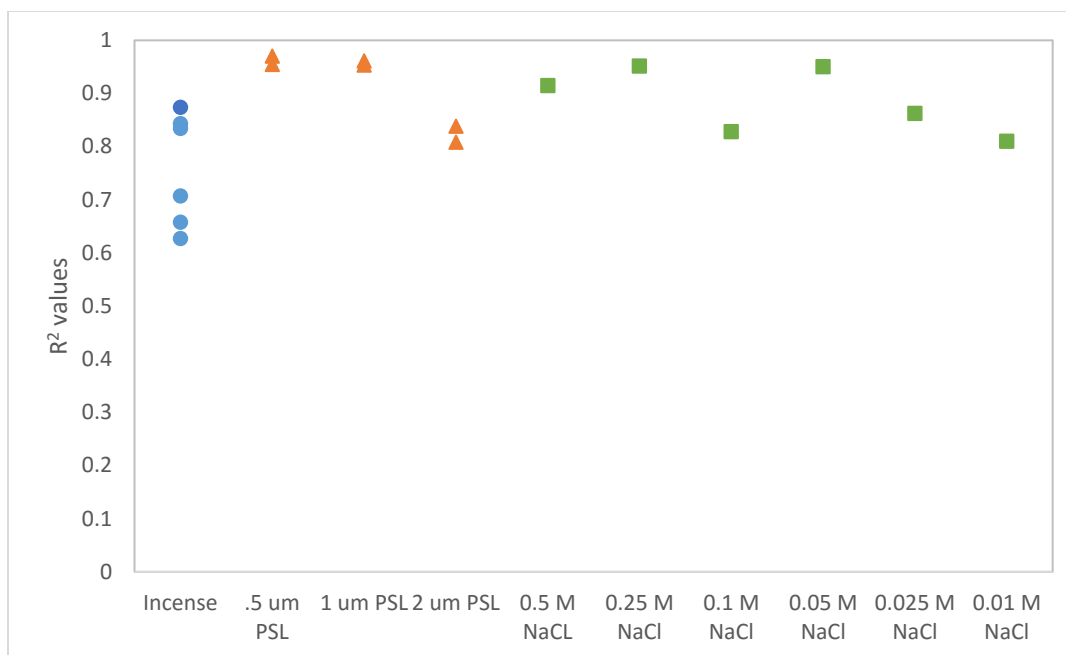


Figure 4.9: Shinyei PD42NS vs. DustTrak R² values

Wang et al. have R² values, when compared to the DustTrak, of 0.95 after adjusting for the curvature of the response at higher concentrations by measuring the response at lower concentrations before the curvature starts.²³ Austin et al had R² values, when compared to a TSI Aerosol Particle Sizer, ranging between 0.66 to 0.99, with lower R² values obtained for smaller particles.²¹ Figure 4.2 shows the Shinyei sensor approaching and exceeding a saturation concentration, which produces a curvature, similar to what is shown in Wang et al.²³ In our experiments, Figure 4.3 shows an R² values of 0.929 for 0.25 M NaCl particles, which is similar to the R² values found in Wang et al.²³ Other experiments, as seen in Figure 4.9, have similar R² values to what is seen in Figure 4.3, with lower particulate sizes having lower R² values, similar to Austin et al.²¹ These R² values achieved in our experiments were higher than what was reported by Bergin et al.

The data also showed variation in the saturation and limits of detection based on the particle type and size, which was also noted by Bergin et al.⁹⁸ Bergin et al. discussed the importance of this variation, since the composition of particulate matter can vary with concentration due to episodic spikes coming from specific point sources. Bergin et al. also notes the bias that a sensor may have based on the particle type it is calibrated with.⁹⁸ PM in the atmosphere derives from various sources and processes, and the response and accuracy of the sensor are sensitive to this variation. Therefore, to accurately measure PM in a given location, a sensor like the Shinyei would need to be calibrated on site with consideration of the particulate compositions there.^{22, 86} This is an important consideration to be addressed if these sensors are going to be deployed for use in multiple locations to determine air quality.^{96, 97}

4.2 Prototype-G – LED Wavelength Variation

The Shinyei PD42NS sensor unit in Prototype-G was modified by replacing the standard infrared LED with a green LED (530 nm). Prototype-G and the standard Shinyei were tested together with incense smoke, PSL, and NaCl. The time series of an NaCl test comparing the sensor with a green LED and a sensor with the standard infrared LED is shown in Figure 4.10. This test was run with a 0.1 M NaCl aqueous concentration, which nominally produces particles of size ~0.1 to 0.3 μm .

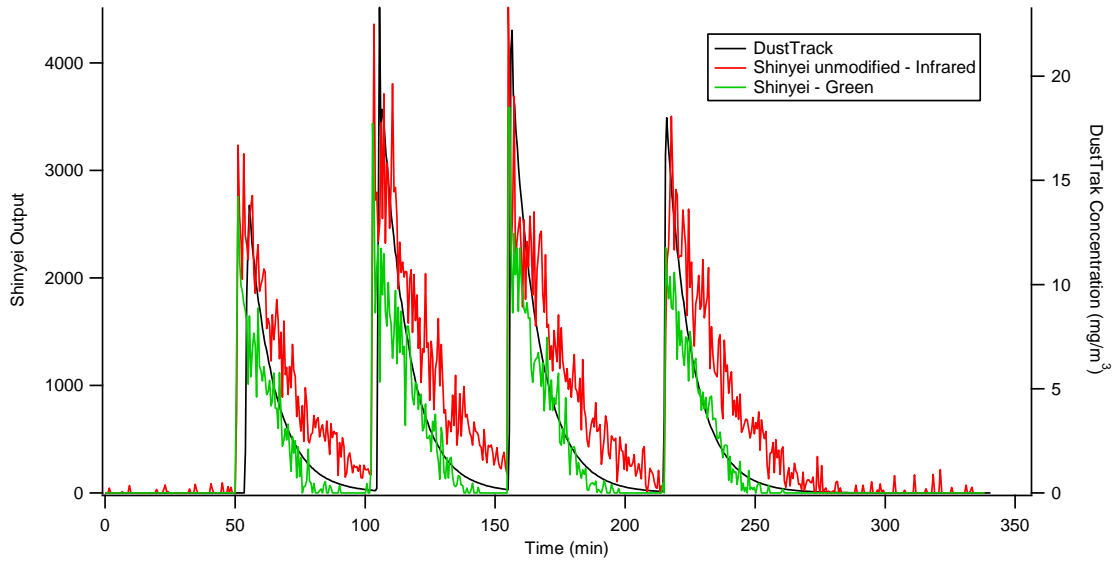


Figure 4.10: Green vs Infrared time series – 0.1 M NaCl

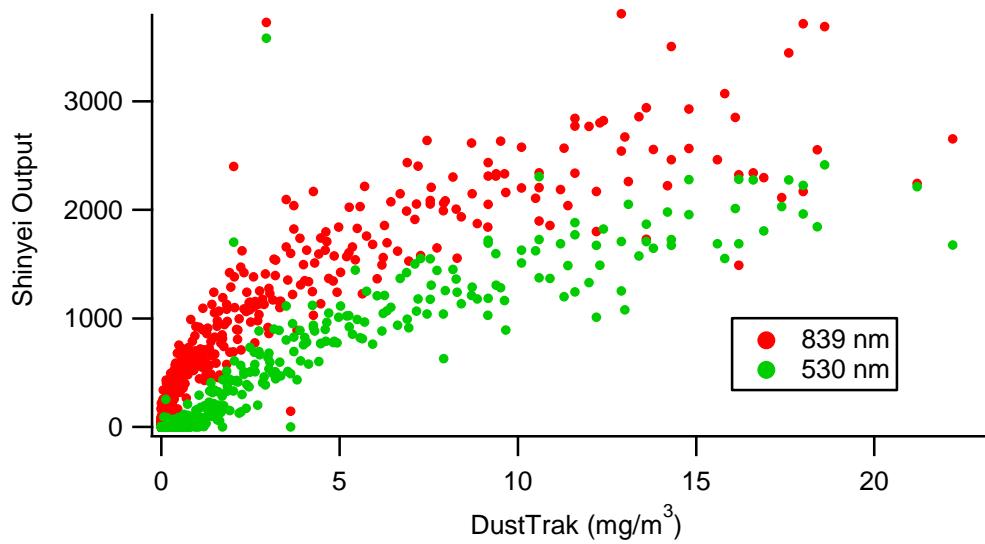


Figure 4.11: Shinyei vs DustTrak – 0.1 M NaCl

In Figure 4.11, it is shown that the unmodified Shinyei had a greater response than Prototype-G, even though the green LED (6.5-7 mW) had greater optical power than the infrared LED (~0.5 mW). The silicon photodiode is less sensitive to lower wavelengths,¹¹² however, the green LED selected for the prototype had a greater power output in an attempt to compensate for this. This indicates that, in addition to

the complex relationship between particle type (refractive index), size, and wavelength, that the sensitivity of the detector to different wavelengths also needs to be considered in the prototype design.

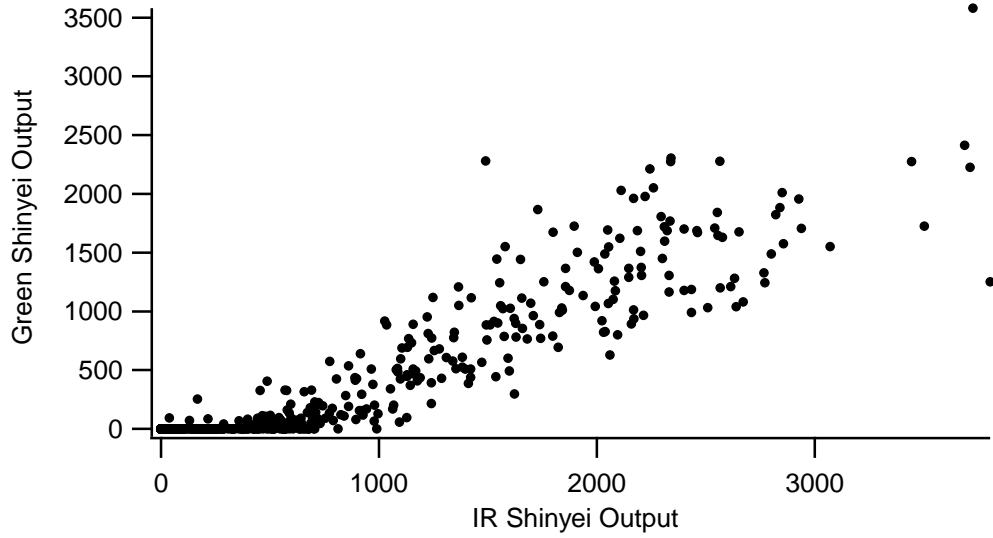


Figure 4.12: Infrared Shinyei output vs green Shinyei output comparison – 0.1 M NaCl

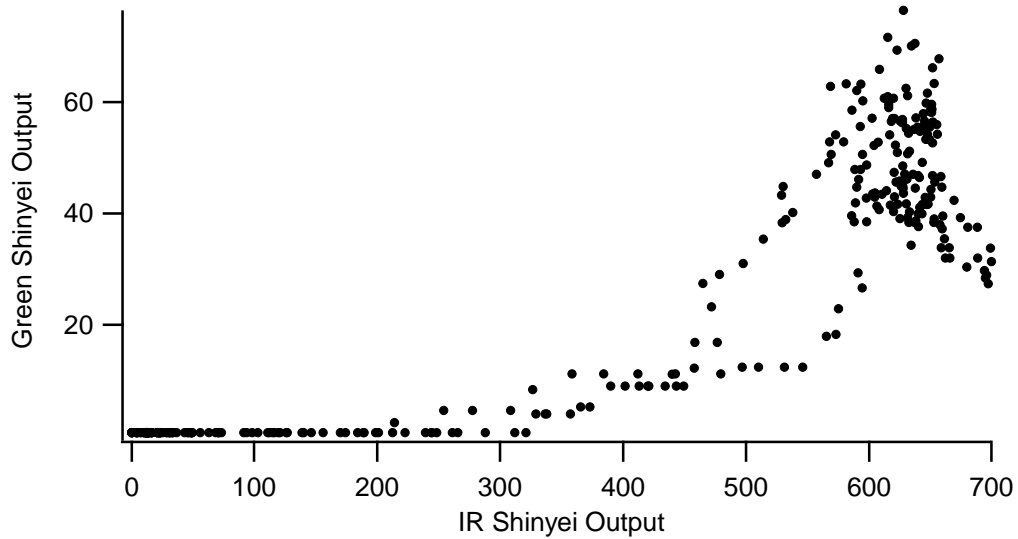


Figure 4.13: Infrared Shinyei output vs green Shinyei output comparison – 1 μm PSL

In Figure 4.12 and Figure 4.13, the Prototype-G data is graphed in relation to the unmodified Shinyei data. Figure 4.12 and Figure 4.13 show that the green LED

has a significantly higher limit of detection than the IR LED. This is likely due to the photodiode not being as sensitive to the green wavelengths, so the threshold is triggered less often and needs higher PM concentrations (about $570 \mu\text{g}/\text{m}^3$ for NaCl and $25 \mu\text{g}/\text{m}^3$ for PSL) to be triggered.

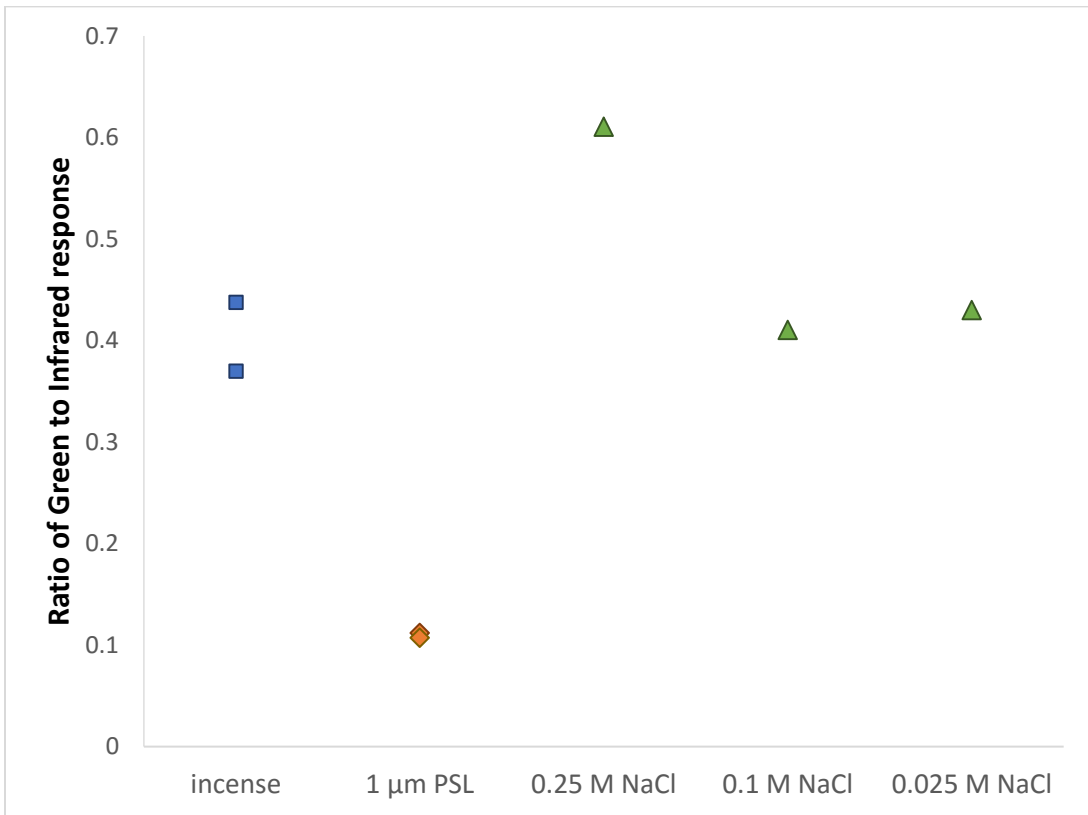


Figure 4.14: Compilation of green response to infrared response – NaCl

Using Figure 4.12 and similar graphs from other experimental runs, the ratio of the response of the green LED versus the response of the infrared LED was determined for incense, NaCl, and PSL microspheres (Figure 4.14). Figure 4.14 shows that the ratio of the green and infrared readings varies based on the various particle types. The lowest ratio was observed for the PSL particles, which had a ratio of about 0.1. The highest ratio was observed for the 0.25 M NaCl, which had a ratio of about 0.6. Therefore, Figure 4.14 suggests that measuring an ambient air sample

with multiple wavelengths can aid in the determination of particulate size and concentration. The variation in wavelengths means that different samples will have a different set of readings based on the wavelengths measured. Since the response of the sensor is dependent on the particulate size, type, and concentration, the measurement of the sample at multiple wavelengths will allow for the determination of these parameters. Theoretically, using three different wavelengths will allow for the determination of the particulate size, and concentration.¹¹³

This is important, since this variation of response based on wavelength can help mitigate the bias mentioned in Bergin et al.⁹⁸ By employing multiple wavelengths, the instrument can be calibrated to identify variations in particle size and concentration. This allows for a single set of calibrations to be used to accurately determine the PM concentration in environments with varying source influences.

4.3 Prototype-R – Potentiometer improvements

For Prototype-R, a potentiometer was added between the threshold pin and the ground pin of the Shinyei sensor. The potentiometer has an adjustable resistance between 0 and 20 k Ω . Using the potentiometer on the prototype, the reference voltage for the P2 comparator was decreased allowing for lower intensities of scattering to be detected. Both Shinyei sensors were modified in this way for testing the ability of the sensor to measure the concentrations of 1 μm PSL microspheres with the potentiometer set at varying resistances (5 k Ω , 10 k Ω , 15 k Ω , and 20 k Ω). The unmodified Shinyei sensor has an 82 k Ω resistor in parallel with the potentiometer. Figure 4.15 shows the time series for an experimental run with 1 μm PSL microspheres. In this sample series, the resistance of the potentiometer was set

to 15 kΩ, which lowers the threshold of the Shinyei sensor allowing for it to detect smaller particles. Our evaluation of Prototype-R shows that decreasing the resistance of the threshold resistor increases the sensitivity of the Shinyei sensor. This response may enable more accurate measurements of air with low PM concentrations.

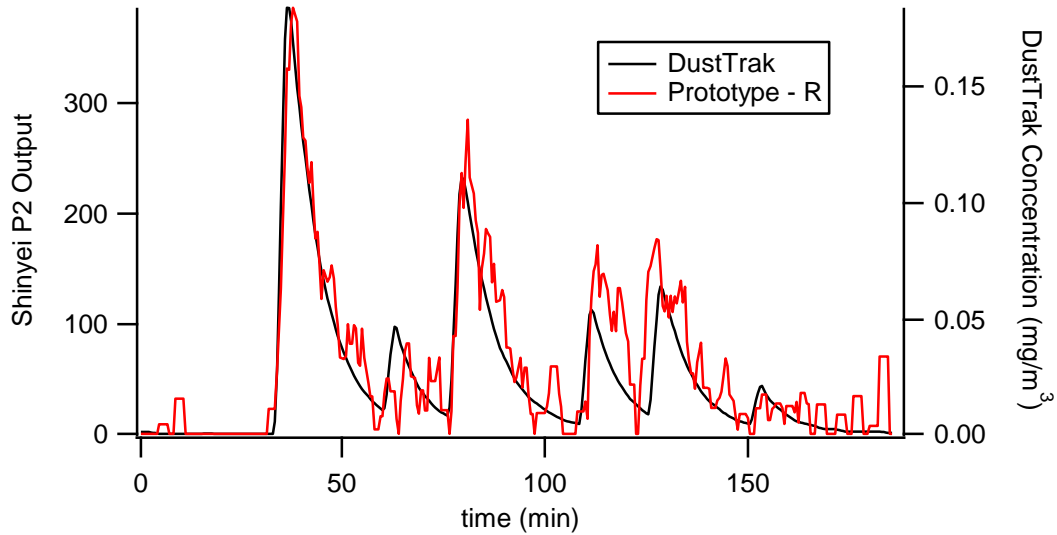


Figure 4.15: Prototype – R 15 kΩ and DustTrak time series – 1 μm PSL

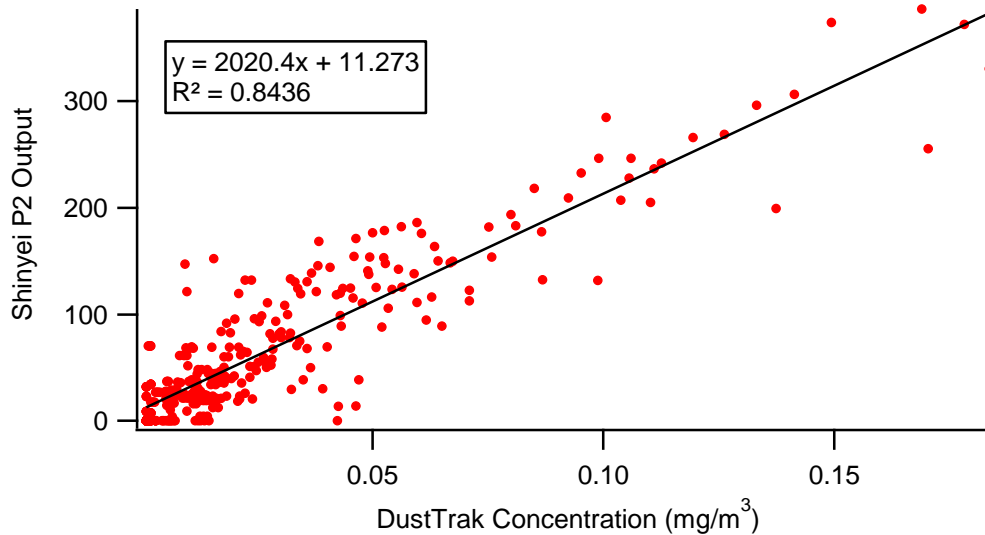


Figure 4.16: DustTrak vs Prototype – R 15 kΩ- 1 μm PSL

In Figure 4.16, the Prototype-R data are graphed in relation to the DustTrak concentration to determine the calibration slope for the Prototype-R at this resistance

setting. In Figure 4.17, the calibration slopes for all the experimental runs are shown in relation to the resistance of the potentiometer. This data is a compilation graph for the 1 μm PSL runs.

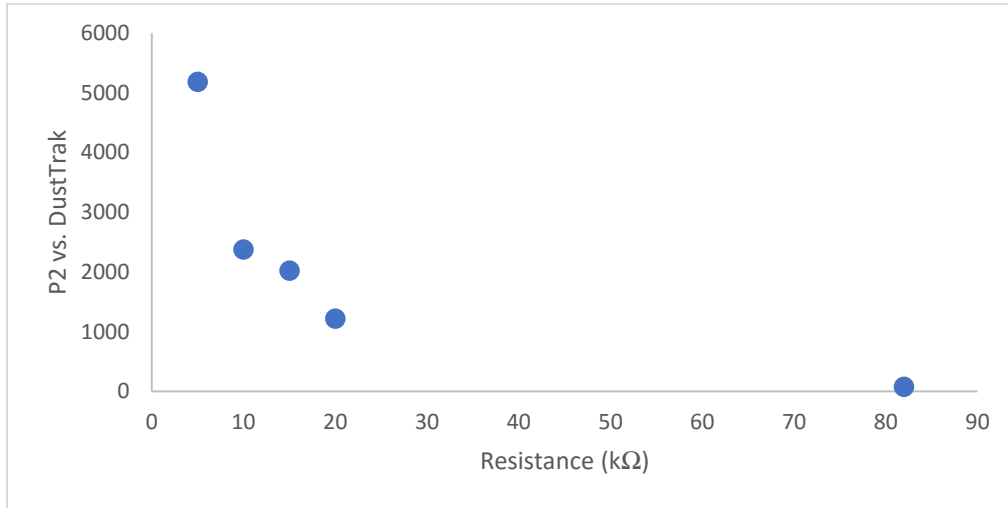


Figure 4.17: Prototype-R response in relation to resistance change – 1 μm PSL microspheres

Figure 4.17 shows that the sensitivity of Prototype-R increases with the decrease in resistance of the potentiometer (which decreases the threshold of detection.) This data shows that lowering the threshold greatly increases the response of the sensor, even for 1 μm particles. However, the noise in the system (noise readings of the P2 signal increased from ranging between 1.45 to 8 times the noise of P1 signal which was unmodified) also increased with the lowering of the threshold. Because of this noise, the signal is not improved and at times decreased due to the increased triggering with no concentration. This implies that when the threshold is lowered the comparator is more easily triggered by the instrument's noise from the ambient light entering the sensor and the scatter of the LED in the sampling chamber.

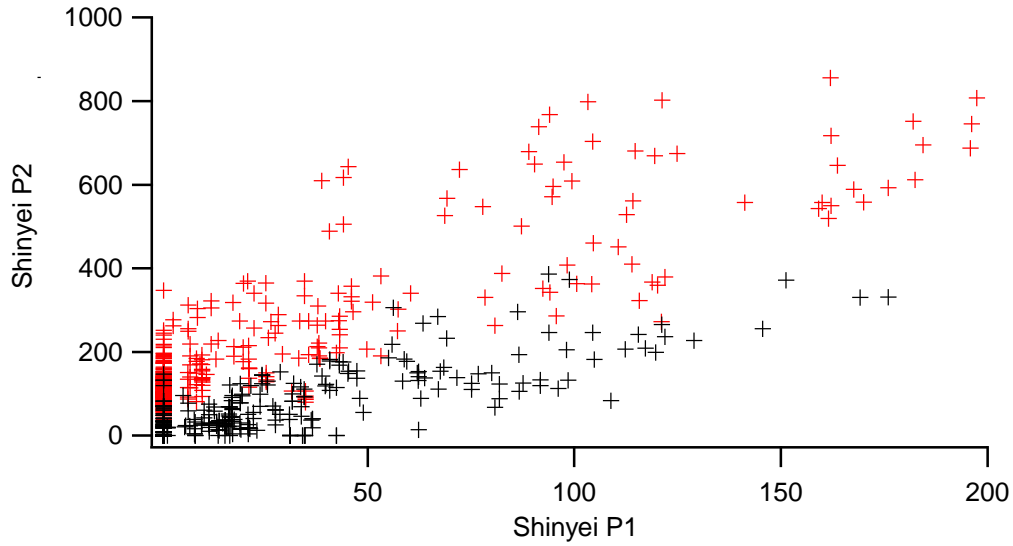


Figure 4.18: P1 vs P2 1 μm PSL – red 5 $\text{k}\Omega$; black 15 $\text{k}\Omega$

In Figure 4.18, the modified P2 output is graphed in relation to the standard P1 output. Similar graphs were used for other resistances and for 0.5 μm PSL. The slopes from the data series of Figure 4.18 and similar graphs are plotted in Figure 4.19 and show the sensors' sensitivity to potentiometer resistance.

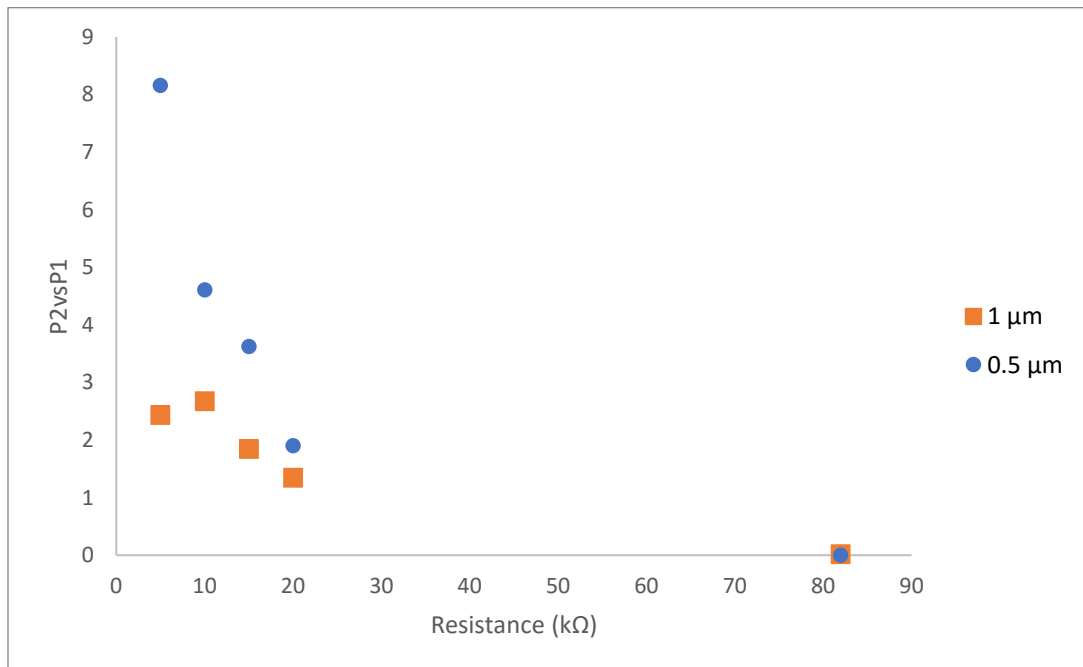


Figure 4.19: PSL Sensitivity Ratio in relation to effective Potentiometer Resistance

The data in Figure 4.19 shows that the response increases with the decrease resistance in the potentiometer. P1 is the unmodified sensor output with the original measurements. P2 is the modified sensor output where the threshold is set by the potentiometer allowing for the lowering or raising of the comparator reference voltage. This graph shows for 1 μm PSL an increase of the response of about three times with the potentiometer set at 10 $\text{k}\Omega$. The response for the 0.5 μm PSL increased greater than the response improvement for the 1 μm PSL. There was significant improvement between 5 $\text{k}\Omega$ and 10 $\text{k}\Omega$. Also, the response increase of 0.5 μm PSL is greater than the response increase of 1 μm PSL. This is most likely due to less of the 0.5 μm PSL particles being detected in the unmodified Shinyei sensor in comparison to the 1 μm PSL.

Sensitivity improvement would need to be accompanied by a decrease in sensor noise. With the lowering of the threshold, the background noise increased between 1.45 to 8 times which inhibited the increase in sensitivity of the Shinyei sensor by decreasing the threshold. If, however, the background noise in the sensor is decreased using other means, such as decreasing the amount of ambient light entering the sensor and the amount of light scattered by the sampling chamber itself, then the sensitivity should be able to be increased with lowering the threshold, since the standard configuration has minimal noise. With a lower background noise, the lower intensities of light scattered would be able to be distinguished and counted, improving the accuracy of the sensor under low PM concentrations.

4.4 Flowrate Comparisons

A comparison of the Shinyei performance with the different methods of sampling was done using 2 µm PSL. The PM concentration was kept at an approximately constant level for approximately a half an hour (28 minutes). The prototype sensor with the fan, prototype with the piezo pump, and an unmodified Shinyei sensor were operated during this run. The DustTrak was also operated as the reference measurement. The fan and the pump were each operated with a flowrate of 0.1 L/min.

The signal to noise ratio used is shown in the equation below.

$$S/N = \frac{\mu}{\sigma}$$

Where S/N is the signal to noise ratio, μ is the measurement mean, and σ is the standard deviation.¹¹⁴ The inconstancy in concentration will increase the standard deviation of all of the sensor data sets will be higher, lowering the signal to noise ratio. The lowering of the signal to noise makes it less likely to find a significant difference due to an increase of noise in the system. The signal to noise ratio was calculated using the half an hour when the PM was kept at a constant level.

The increase in flow rate is shown to have minimal increase in signal to noise ratio. The unmodified Shinyei sensor had a signal to noise ratio of 4.07; the Shinyei changed with a fan has a signal to noise ratio of 3.94; the shinyei modified with a pump had a signal to noise ratio of 8.65. These differences with the fan to unmodified were not statistically significant at the 95% confidence interval using a one tailed probability density function; the pump however was statistically significant at a 95% confidence interval.¹¹⁵ The fan showed no significant change in the signal

to noise ratio and the pump showed a minimal difference to an increase in signal to noise ratio. Figure 4.20 shows a time series of the measurements for this experiment.

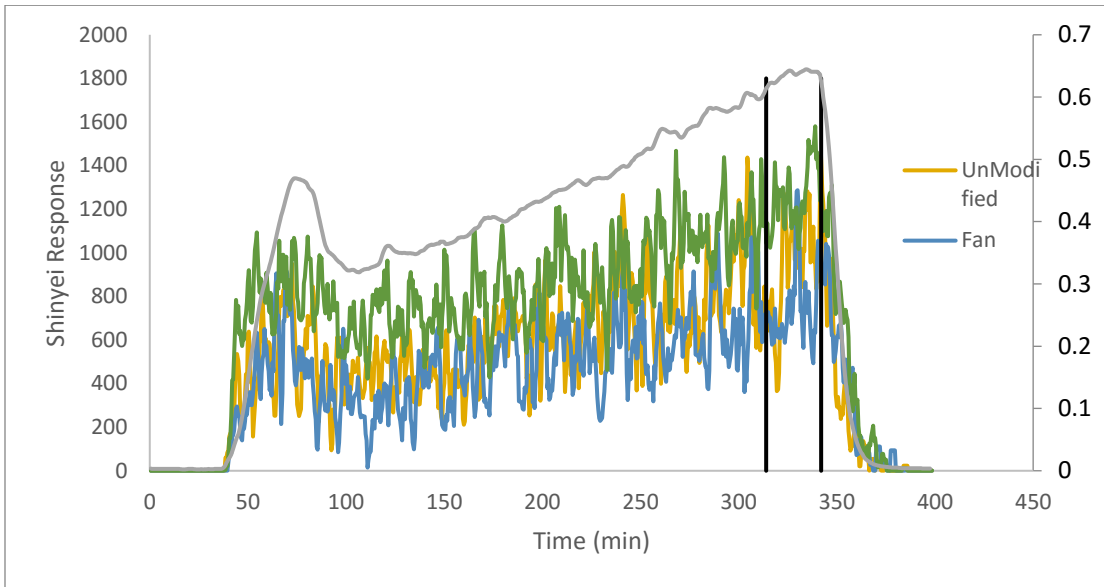


Figure 4.20: Time series of the experiment run with $2\ \mu\text{m}$ PSL to compare the Shinyei response under different flow configurations.

The results with a minimal change in signal-to-noise ratio between the different sensors show the ability to use a pump or a fan as a source of flow. The use of a pump or a fan will improve the usage of the sensor since the alignment of the sensor will no longer be important, allowing for wearable use. The pump and the fan are being considered for use in the novel sensor, as they will enable the sensor to be worn and to provide accurate measurements of the PM concentrations, even if the sensor is moving. The unmodified Shinyei is highly sensitive to movement, giving high background readings when the Shinyei sensor is touched. We hypothesize that the use of a fan or a pump will help mediate this sensitivity. Also, the unmodified Shinyei is sensitive to wind,¹¹⁶ likely because the flow provided by the heated resistor is quite weak. In attempts to measure the flowrate coming from the base Shinyei with the heated resistor, the flows were too low to get an estimate of the flowrate. The

increased flowrate from a fan or pump will reduce the influence of wind on the sensor response.¹¹⁶

4.5 Shinyei stability with Time

A major question about the use of low-cost sensors is their stability over time and the appropriate frequency of calibration. We investigated the stability of the Shinyei over time by comparing experiments with identical PM run months apart. For 1 μ m PSL experiments run ~4 months apart, there was a significant decrease in the Shinyei response. Figure 4.8 shows excellent repeatability of the Shinyei sensor for experiments run in close succession (within days or weeks), especially for PSL. The comparison in Fig. 4.21 shows that there is a reduction in detection with time. This reduction is likely due to contamination of the photodiode and/or LED from accumulated usage. This could lead to reduced light detection for similar particles, leading to lower readings for a given concentration.

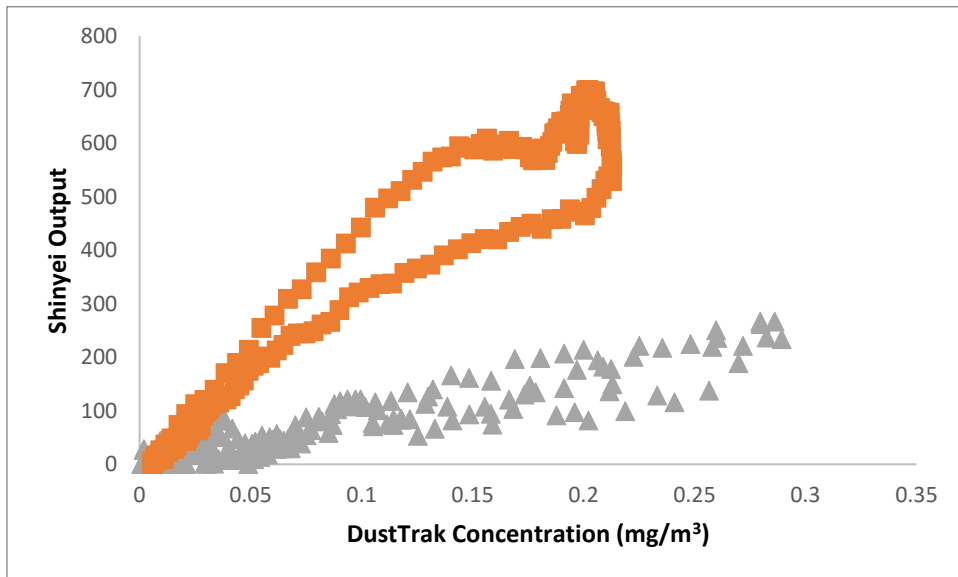


Figure 4.21: Variation in response with time – 1 μ m PSL

This variation suggests that the Shinyei sensor may need to be cleaned regularly, since there were about 4 months difference in time between these runs. This shows a clear decline in response with heavy use. A more systematic study would be needed to recommend the timing of such cleaning or recalibrations.

4.6 Simulation results

Mie Plot 4600 was used to provide a theoretical basis for the prototype design, and specifically, the orientation of the photodetector. This simulation utilizes the BHMIE algorithm developed by Bohrem and Huffmann.⁸⁰ Wavelength, particle size, refractive index, and scattering angle were varied to determine the ideal angle for the photodiode where the scatter intensity is the greatest. The values used in the simulation are shown in Table 4.1.

Table 4.1: Parameters varied in the Mie simulations

Parameter	Values
Wavelength (nm)	400, 530, 650
Particle Size (μm)	10, 5, 2.5, 1, 0.5, 0.25
Refractive Index (n)	1.45, 1.5, 1.54
Scattering angle (θ)	25, 45, 120, 140, 150

Our objective is to build the final prototype with all three wavelengths for measurement. Particle size and refractive index variation simulates the variation in particles likely to be encountered in an ambient deployment. These simulations help to determine the best scattering angle and how different wavelengths interact with varying particle types.

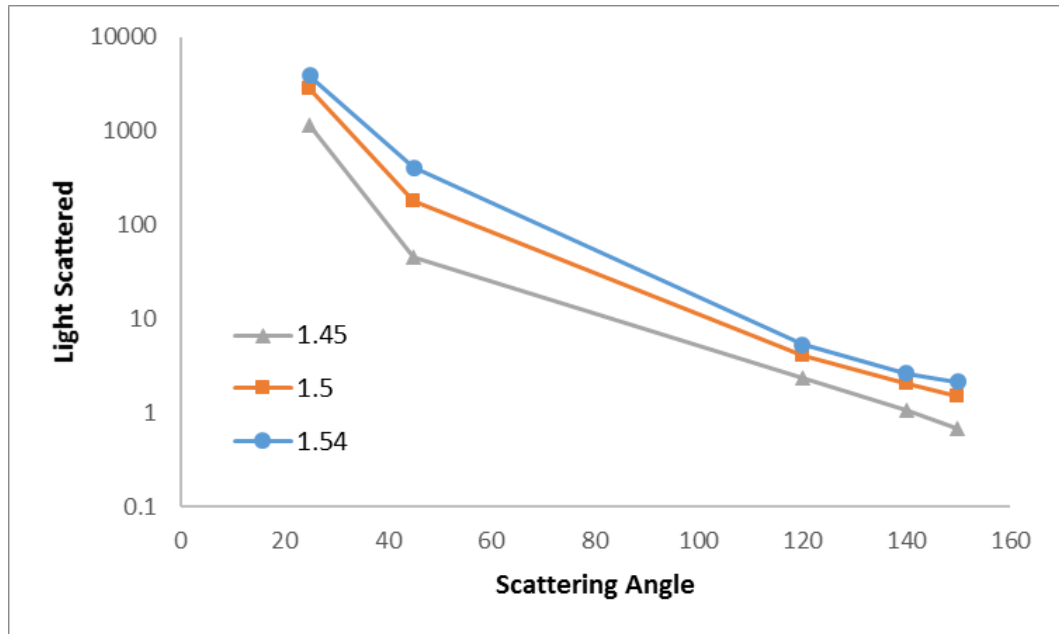


Figure 4.22: Variation in scattering intensity over scattering angle and refractive index

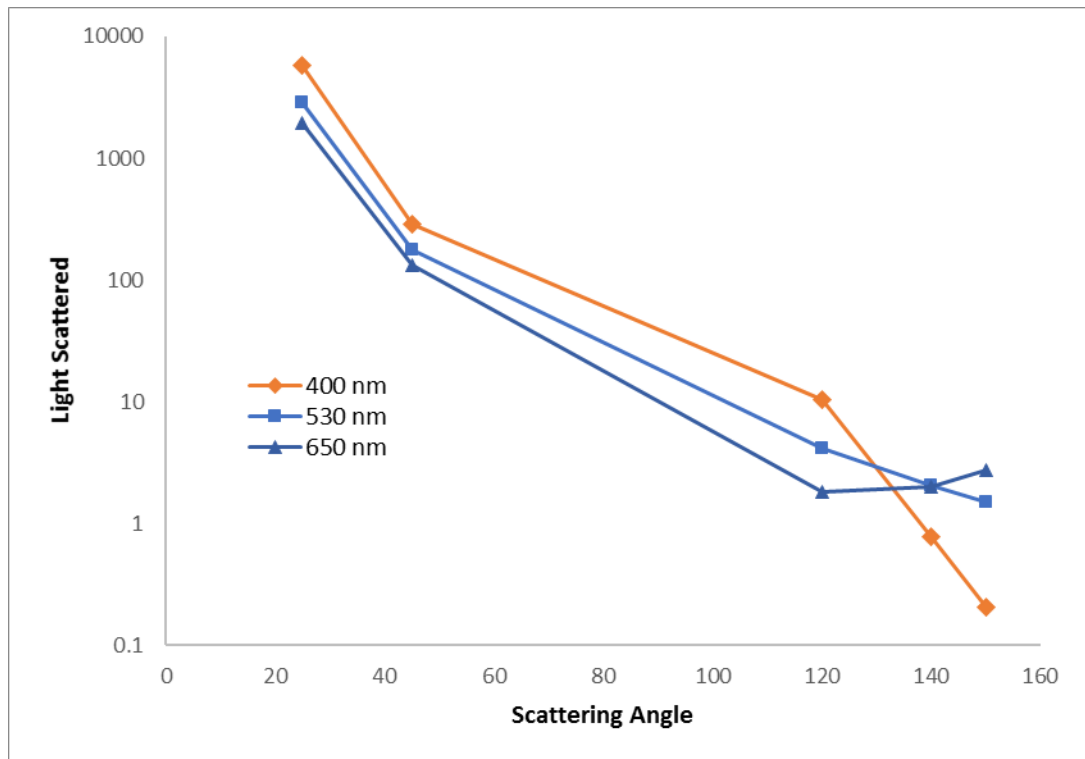


Figure 4.23: Variation in scattering intensity over scattering angle and wavelength

Figure 4.22 and Figure 4.23 show an increase in scattering intensity with at lower scattering angles due to the prominence of forward scattering by these particles. The figures show that the forward scattering has higher intensities across varying refractive indexes and wavelengths. This trend is consistent across the different simulations. These graphs show the importance of a low scattering angle with an increase in the magnitude of the scattering is greatly increased at the 45° and 25° scattering angle. Therefore, the prototype sensor would be optimized with the photodiode positioned to maximize the detection of the forward scattered light.

5.0 Conclusion

The Shinyei PD42NS sensor was calibrated across various particle types and sizes, and the effects of wavelength, threshold, and flow modifications were investigated. The response of the Shinyei varied significantly based on the size and the type of particles measured. The modification of wavelength and threshold gave promising results, which will be considered in the design of the prototype sensor for the determination of particle size and composition. The modification of airflow showed only modest improvement, but demonstrated the utility of two different approaches for dynamic sampling under a wearable configuration.

First, the response of the Shinyei PD42NS is highly dependent on the particle size and type, in addition to concentration. The sensor has a higher response to larger particles compared to small particles for the same mass concentration. The sensor also has an increased sensitivity to NaCl compared with PSL for the same size and concentration, due to differences in refractive index. This means that to know the concentration, one must know physical characteristics of the particle size distribution. This indicates that the base Shinyei sensor cannot be deployed for accurate PM measurements as a stand-alone instrument. With the requirement for co-deployment of higher-cost instruments, it has limited applications due to the need to know the physical characteristics of the particles being measured. This leads to questions of the accuracy across multiple environments where the PM type and sizes vary in space and time.

Our testing with LEDs of different wavelengths showed that the sensitivity to particle size and composition varies by wavelength, consistent with predictions by Mie theory. This variation by wavelength means that the variations of particle size and composition will result in different sensor responses across with different wavelengths. Therefore, using multiple wavelengths can provide a more accurate understanding of the particulate concentrations. Due to this variation, the novel sensor will utilize three wavelengths to inform the particle size and concentration.

Lowering the threshold of the Shinyei PD42NS sensor improved the response of the sensor's P2 detection channel. The response to 0.5 μm particles was greatly increased over 1 μm particles by lowering the threshold. This threshold modulation allows for improvements in detecting particles, especially those with smaller diameters. However, background noise also increased with the lower threshold setting, leading to higher limits of detection. Thus, the improvements in sensitivity were offset by the higher background noise, suggesting a difficult tradeoff common to many analytical instruments.

Lastly, when flow rate variation was investigated using either a pump or fan, the increase in the rate of air flow was found to have an insignificant impact on the sensitivity of Shinyei. Even though there was no significant increase in instrument's sensitivity, the pump or the fan will maintain a constant airflow through the sensor chamber regardless of orientation and should allow for the sensor to operate in variable orientations. For a wearable sensor, orientation can vary based on what the person is doing and a heavy reliance on orientation will skew measurements when the

instrument is not in the optimal alignment. This demonstrates that the fan or the pump can provide good sampling efficacy for the prototype design.

5.1 Future Work

To improve the characterization of the Shinyei sensor, the Shinyei sensor should be calibrated with 0.75, 3, and 6 μm PSL to provide direct comparisons with the work of Austin et al.²¹ The Shinyei sensor should also be calibrated with sucrose and ammonium nitrate with similar sizes to the sodium chloride runs to directly compare with the work of Wang et al.²³ For ambient monitoring, the Shinyei sensor should be calibrated with ambient air at varying locations and varying seasons to be able to see the variation in the calibration throughout the year to better understand how accurate the Shinyei sensor will be for ambient monitoring.

To improve on the testing of modifications, first the Shinyei sensor should be tested with more LED wavelengths to better understand how the sensor varies in relation to wavelength and composition. This change will help inform how varying wavelengths will help determine the concentration of the particulate matter with varying composition and size. For the threshold modulation, the Shinyei sensor's sampling chamber should be darkened to reduce noise within the chamber. Once the noise is reduced the sensor should be tested across the varying thresholds to look for improvements to signal with a lower background noise.

The next step of the project is constructing a novel prototype sensor based upon the results from the modifications testing on the Shinyei sensor. Indeed, several prototypes have already been constructed and tested, although many modifications to

these sensors are needed. From the variation of the response with the green LED, the prototype will employ three different wavelengths for the measurement. From the testing of the pump and the fan, the prototype will use a pump or a fan, since these methods of flow did not negatively affect the measurements. This prototype will be constructed in the lab with a custom sampling chamber and a custom circuit board. The prototype will have a photodiode positioned to detect scattered light at an angle between 25-45° and utilize a low-power laser to decrease noise from the light dispersion. The sampling chamber will be painted optical black to prevent backscatter from the chamber walls to reduce the background noise under low PM concentrations.

This sensor will then need to be tested and modified to further optimize the design of the sensor. Once the final design is created, it will be calibrated using various particle types and sizes. This testing and calibration will prepare the sensor to be used in ambient measurements. The new sensor would be able to be calibrated using the particles used in the Shinyei characterization section along with ammonia nitrate, sucrose, and ambient particulate matter.

The sensor will also integrate a collection device for the collection of larger particles, similar to Novosselov et al.¹¹⁷ The chamber will collect particulates that are larger than 1 µm in diameter. These particles can be analyzed off line, for example, they can be characterized for allergens and other particle types that are more specific triggers for asthma.

Once the sensor is complete and ready for deployment, the sensor will be sent to Southern Methodist University for use in pediatric asthma research. This sensor will be worn by a cohort of children with pediatric asthma to investigate further the environmental triggers of pediatric asthma. This sensor can also be used in other research studies investigating the health effects of particulate matter exposure.

References

1. Statistics, N. C. f. H., National Health Interview Survey. In Health, N. C. f. E., Ed. Center for Disease Control: <https://www.cdc.gov/asthma/nhis/>, 2016.
2. Iordanidou, M.; Loukides, S.; Paraskakis, E., Asthma phenotypes in children and stratified pharmacological treatment regimens. *Expert Review of Clinical Pharmacology* **2017**, *10*, (3), 293-303.
3. Asthma, G. I. f., Global Strategy for Asthma Management and Prevention. In www.ginasthma.org, 2017.
4. Lin, M. C., Y Burnett, RT Villeneuve, PJ Kerwski, D, The Influence of Ambient Coarse Particulate Matter on Asthma Hospitalization in Children: case-crossover and time-series analyses In *Environ Health Perspect.* : 2002 Vol. 110, pp 575-581.
5. Sbihi, H.; Koehoorn, M.; Tamburic, L.; Brauer, M., Asthma Trajectories in a Population-based Birth Cohort. Impacts of Air Pollution and Greenness. *American Journal of Respiratory and Critical Care Medicine* **2017**, *195*, (5), 607-613.
6. Khreis, H.; Kelly, C.; Tate, J.; Parslow, R.; Lucas, K.; Nieuwenhuijsen, M., Exposure to traffic-related air pollution and risk of development of childhood asthma: A systematic review and meta-analysis. *Environment International* **2017**, *100*, 1-31.
7. Ellwood, P.; Asher, M. I.; Billo, N. E.; Bissell, K.; Chiang, C. Y.; Ellwood, E. M.; El-Sony, A.; Garcia-Marcos, L.; Mallol, J.; Marks, G. B.; Pearce, N. E.; Strachan, D. P., The Global Asthma Network rationale and methods for Phase I global surveillance: prevalence, severity, management and risk factors. *European Respiratory Journal* **2017**, *49*, (1), 6.
8. Barnett, A. G.; Williams, G. M.; Schwartz, J.; Neller, A. H.; Best, T. L.; Petroschevsky, A. L.; Simpson, R. W., Air pollution and child respiratory health - A case-crossover study in Australia and new Zealand. *American Journal of Respiratory and Critical Care Medicine* **2005**, *171*, (11), 1272-1278.
9. Gautier, C.; Charpin, D., Environmental triggers and avoidance in the management of asthma. *Journal of Asthma and Allergy* **2017**, *10*, 47-56.
10. Megido, L.; Negral, L.; Castrillon, L.; Fernandez-Nava, Y.; Suarez-Pena, B.; Maranon, E., Impact of secondary inorganic aerosol and road traffic at a suburban air quality monitoring station. *Journal of Environmental Management* **2017**, *189*, 36-45.
11. Rathnayake, C. M.; Metwali, N.; Jayarathne, T.; Kettler, J.; Huang, Y. F.; Thorne, P. S.; O'Shaughnessy, P. T.; Stone, E. A., Influence of rain on the abundance of bioaerosols in fine and coarse particles. *Atmospheric Chemistry and Physics* **2017**, *17*, (3), 2459-2475.
12. Steinle, S.; Reis, S.; Sabel, C. E.; Semple, S.; Twigg, M. M.; Braban, C. F.; Leeson, S. R.; Heal, M. R.; Harrison, D.; Lin, C.; Wu, H., Personal exposure monitoring of PM_{2.5} in indoor and outdoor microenvironments. *Science of the Total Environment* **2015**, *508*, 383-394.
13. Apte, J. S.; Messier, K. P.; Gani, S.; Brauer, M.; Kirchstetter, T. W.; Lunden, M. M.; Marshall, J. D.; Portier, C. J.; Vermeulen, R. C. H.; Hamburg, S. P., High-Resolution Air Pollution Mapping with Google Street View Cars: Exploiting Big Data. *Environmental Science & Technology* **2017**.

14. Berghmans, P.; Bleux, N.; Panis, L. I.; Mishra, V. K.; Torfs, R.; Van Poppel, M., Exposure assessment of a cyclist to PM10 and ultrafine particles. *Science of the Total Environment* **2009**, *407*, (4), 1286-1298.
15. Ch, S. D.; Gokhale, S., Monitoring and Assessment of O-3 and PM1 in the Microenvironment of a Workplace. *Environmental Modeling & Assessment* **2015**, *20*, (5), 521-534.
16. Mar, T. F.; Koenig, J. Q.; Primomo, J., Associations between asthma emergency visits and particulate matter sources, including diesel emissions from stationary generators in Tacoma, Washington. *Inhalation Toxicology* **2010**, *22*, (6), 445-448.
17. Rault, T.; Bouabdallah, A.; Challal, Y.; Marin, F., A survey of energy-efficient context recognition systems using wearable sensors for healthcare applications. *Pervasive and Mobile Computing* **2017**, *37*, 23-44.
18. Rohit, F.; Kulathumani, V.; Kavi, R.; Elwarfalli, I.; Kecojevic, V.; Nimbarte, A., Real-time drowsiness detection using wearable, lightweight brain sensing headbands. *Iet Intelligent Transport Systems* **2017**, *11*, (5), 255-263.
19. Sheykhi, S.; Mosca, L.; Anzenbacher, P., Toward wearable sensors: optical sensor for detection of ammonium nitrate-based explosives, ANFO and ANNM. *Chemical Communications* **2017**, *53*, (37), 5196-5199.
20. Xu, Z. H.; Liu, Y. C.; Williams, I.; Li, Y.; Qian, F. Y.; Wang, L.; Lei, Y.; Li, B. K., Flat enzyme-based lactate biofuel cell integrated with power management system: Towards long term in situ power supply for wearable sensors. *Applied Energy* **2017**, *194*, 71-80.
21. Austin, E.; Novosselov, I.; Seto, E.; Yost, M. G., Laboratory Evaluation of the Shinyei PPD42NS Low-Cost Particulate Matter Sensor (vol 10, e0137789, 2015). *Plos One* **2015**, *10*, (10).
22. Holstius, D. M.; Pillarisetti, A.; Smith, K. R.; Seto, E., Field calibrations of a low-cost aerosol sensor at a regulatory monitoring site in California. *Atmospheric Measurement Techniques* **2014**, *7*, (4), 1121-1131.
23. Wang, Y.; Li, J. Y.; Jing, H.; Zhang, Q.; Jiang, J. K.; Biswas, P., Laboratory Evaluation and Calibration of Three Low-Cost Particle Sensors for Particulate Matter Measurement. *Aerosol Science and Technology* **2015**, *49*, (11), 1063-1077.
24. United States. Congress. House. Committee on Interstate and Foreign Commerce., *Clean air act amendments of 1970; report (to accompany H.R. 17255)*. Washington., 1970; p 53 p.
25. Seinfeld, J.; Pandis, S., *Atmospheric Chemistry and Physics: From Air Pollution to Climate Change*. John Wiley & Sons, Inc: New York, NY 1998.
26. Squizzato, S.; Cazzaro, M.; Innocente, E.; Visin, F.; Hopke, P. K.; Rampazzo, G., Urban air quality in a mid-size city - PM2.5 composition, sources and identification of impact areas: From local to long range contributions. *Atmospheric Research* **2017**, *186*, 51-62.
27. Edgerton, E. S.; Hartsell, B. E.; Saylor, R. D.; Jansen, J. J.; Hansen, D. A.; Hidy, G. M., The Southeastern Aerosol Research and Characterization Study, part 3: Continuous measurements of fine particulate matter mass and composition. *Journal of the Air & Waste Management Association* **2006**, *56*, (9), 1325-1341.

28. Habilomatis, G.; Chaloulakou, A., Ultrafine particles dispersion modeling in a street canyon: Development and evaluation of a composite lattice Boltzmann model. *Science of the Total Environment* **2013**, *463*, 478-487.
29. Li, R.; Fu, H. B.; Hu, Q. Q.; Li, C. L.; Zhang, L. W.; Chen, J. M.; Mellouki, A. W., Physiochemical characteristics of aerosol particles in the typical microenvironment of hospital in Shanghai, China. *Science of the Total Environment* **2017**, *580*, 651-659.
30. Zereini, F.; Alt, F.; Messerschmidt, J.; Wiseman, C.; Feldmann, I.; Von Bohlen, A.; Muller, J.; Liebl, K.; Puttmann, W., Concentration and distribution of heavy metals in urban airborne particulate matter in Frankfurt am main, Germany. *Environmental Science & Technology* **2005**, *39*, (9), 2983-2989.
31. Code of Federal Regulations. Title 40. In Counterpoint Pub.: Cambridge, MA, pp CD-ROMs.
32. World Health Organization., *Air quality guidelines : global update 2005 : particulate matter, ozone, nitrogen dioxide, and sulfur dioxide*. World Health Organization: Copenhagen, Denmark, 2006; p ix, 484 p.
33. Baxter, L. K.; Crooks, J. L.; Sacks, J. D., Influence of exposure differences on city-to-city heterogeneity in PM_{2.5}-mortality associations in US cities. *Environmental Health* **2017**, *16*, 8.
34. Barnett, A. G.; Williams, G. M.; Schwartz, J.; Best, T. L.; Neller, A. H.; Petroschevsky, A. L.; Simpson, R. W., The effects of air pollution on hospitalizations for cardiovascular disease in elderly people in Australian and New Zealand cities. *Environmental Health Perspectives* **2006**, *114*, (7), 1018-1023.
35. Branis, M.; Kolomaznikova, J., Monitoring of long-term personal exposure to fine particulate matter (PM_{2.5}). *Air Quality Atmosphere and Health* **2010**, *3*, (4), 235-243.
36. Brook, R. D.; Shin, H. H.; Bard, R. L.; Burnett, R. T.; Vette, A.; Croghan, C.; Thornburg, J.; Rodes, C.; Williams, R., Exploration of the Rapid Effects of Personal Fine Particulate Matter Exposure on Arterial Hemodynamics and Vascular Function during the Same Day. *Environmental Health Perspectives* **2011**, *119*, (5), 688-694.
37. Correia, A. W.; Pope, C. A.; Dockery, D. W.; Wang, Y.; Ezzati, M.; Dominici, F., Effect of Air Pollution Control on Life Expectancy in the United States An Analysis of 545 US Counties for the Period from 2000 to 2007. *Epidemiology* **2013**, *24*, (1), 23-31.
38. Hong, Y. C.; Lee, J. T.; Kim, H.; Ha, E. H.; Schwartz, J.; Christiani, D. C., Effects of air pollutants on acute stroke mortality. *Environmental Health Perspectives* **2002**, *110*, (2), 187-191.
39. Honkoop, P. J.; Simpson, A.; Bonini, M.; Snoeck-Stroband, J. B.; Meah, S.; Chung, K. F.; Usmani, O. S.; Fowler, S.; Sont, J. K., MyAirCoach: the use of home-monitoring and mHealth systems to predict deterioration in asthma control and the occurrence of asthma exacerbations; study protocol of an observational study. *Bmj Open* **2017**, *7*, (1), 8.
40. Hsiao, W. L. W.; Mo, Z. Y.; Fang, M.; Shi, X. M.; Wang, F., Cytotoxicity of PM_{2.5} and PM_{2.5-10} ambient air pollutants assessed by the MTT and the Comet assays. *Mutation Research-Genetic Toxicology and Environmental Mutagenesis* **2000**, *471*, (1-2), 45-55.

41. Huang, K. L.; Liu, S. Y.; Chou, C. C. K.; Lee, Y. H.; Cheng, T. J., The effect of size-segregated ambient particulate matter on Th1/Th2-like immune responses in mice. *Plos One* **2017**, *12*, (2), 16.
42. Langley-Turnbaugh, S. J.; Gordon, N. R.; Lambert, T., Airborne particulates and asthma: a Maine case study. *Toxicology and Industrial Health* **2005**, *21*, (3-4), 75-92.
43. Lim, S. S.; Vos, T.; Flaxman, A. D.; Danaei, G.; Shibuya, K.; Adair-Rohani, H.; Amann, M.; Anderson, H. R.; Andrews, K. G.; Aryee, M.; Atkinson, C.; Bacchus, L. J.; Bahalim, A. N.; Balakrishnan, K.; Balmes, J.; Barker-Collo, S.; Baxter, A.; Bell, M. L.; Blore, J. D.; Blyth, F.; Bonner, C.; Borges, G.; Bourne, R.; Boussinesq, M.; Brauer, M.; Brooks, P.; Bruce, N. G.; Brunekreef, B.; Bryan-Hancock, C.; Bucello, C.; Buchbinder, R.; Bull, F.; Burnett, R. T.; Byers, T. E.; Calabria, B.; Carapetis, J.; Carnahan, E.; Chafe, Z.; Charlson, F.; Chen, H. L.; Chen, J. S.; Cheng, A. T. A.; Child, J. C.; Cohen, A.; Colson, K. E.; Cowie, B. C.; Darby, S.; Darling, S.; Davis, A.; Degenhardt, L.; Dentener, F.; Des Jarlais, D. C.; Devries, K.; Dherani, M.; Ding, E. L.; Dorsey, E. R.; Driscoll, T.; Edmond, K.; Ali, S. E.; Engell, R. E.; Erwin, P. J.; Fahimi, S.; Falder, G.; Farzadfar, F.; Ferrari, A.; Finucane, M. M.; Flaxman, S.; Fowkes, F. G. R.; Freedman, G.; Freeman, M. K.; Gakidou, E.; Ghosh, S.; Giovannucci, E.; Gmel, G.; Graham, K.; Grainger, R.; Grant, B.; Gunnell, D.; Gutierrez, H. R.; Hall, W.; Hoek, H. W.; Hogan, A.; Hosgood, H. D.; Hoy, D.; Hu, H.; Hubbell, B. J.; Hutchings, S. J.; Ibeanusi, S. E.; Jacklyn, G. L.; Jasrasaria, R.; Jonas, J. B.; Kan, H. D.; Kanis, J. A.; Kassebaum, N.; Kawakami, N.; Khang, Y. H.; Khatibzadeh, S.; Khoo, J. P.; Kok, C.; Laden, F.; Lalloo, R.; Lan, Q.; Lathlean, T.; Leasher, J. L.; Leigh, J.; Li, Y.; Lin, J. K.; Lipshultz, S. E.; London, S.; Lozano, R.; Lu, Y.; Mak, J.; Malekzadeh, R.; Mallinger, L.; Marcenes, W.; March, L.; Marks, R.; Martin, R.; McGale, P.; McGrath, J.; Mehta, S.; Mensah, G. A.; Merriman, T. R.; Micha, R.; Michaud, C.; Mishra, V.; Hanafiah, K. M.; Mokdad, A. A.; Morawska, L.; Mozaffarian, D.; Murphy, T.; Naghavi, M.; Neal, B.; Nelson, P. K.; Nolla, J. M.; Norman, R.; Olives, C.; Omer, S. B.; Orchard, J.; Osborne, R.; Ostro, B.; Page, A.; Pandey, K. D.; Parry, C. D. H.; Passmore, E.; Patra, J.; Pearce, N.; Pelizzari, P. M.; Petzold, M.; Phillips, M. R.; Pope, D.; Pope, C. A.; Powles, J.; Rao, M.; Razavi, H.; Rehfuess, E. A.; Rehm, J. T.; Ritz, B.; Rivara, F. P.; Roberts, T.; Robinson, C.; Rodriguez-Portales, J. A.; Romieu, I.; Room, R.; Rosenfeld, L. C.; Roy, A.; Rushton, L.; Salomon, J. A.; Sampson, U.; Sanchez-Riera, L.; Sanman, E.; Sapkota, A.; Seedat, S.; Shi, P. L.; Shield, K.; Shivakoti, R.; Singh, G. M.; Sleet, D. A.; Smith, E.; Smith, K. R.; Stapelberg, N. J. C.; Steenland, K.; Stockl, H.; Stovner, L. J.; Straif, K.; Straney, L.; Thurston, G. D.; Tran, J. H.; Van Dingenen, R.; van Donkelaar, A.; Veerman, J. L.; Vijayakumar, L.; Weintraub, R.; Weissman, M. M.; White, R. A.; Whiteford, H.; Wiersma, S. T.; Wilkinson, J. D.; Williams, H. C.; Williams, W.; Wilson, N.; Woolf, A. D.; Yip, P.; Zielinski, J. M.; Lopez, A. D.; Murray, C. J. L.; Ezzati, M., A comparative risk assessment of burden of disease and injury attributable to 67 risk factors and risk factor clusters in 21 regions, 1990-2010: a systematic analysis for the Global Burden of Disease Study 2010. *Lancet* **2012**, *380*, (9859), 2224-2260.
44. McGee, J. K.; Chen, L. C.; Cohen, M. D.; Chee, G. R.; Prophete, C. M.; Haykal-Coates, N.; Wasson, S. J.; Conner, T. L.; Costa, D. L.; Gavett, S. H.,

- Chemical analysis of World Trade Center fine particulate matter for use in toxicologic assessment. *Environmental Health Perspectives* **2003**, *111*, (7), 972-980.
45. Michikawa, T.; Ueda, K.; Takeuchi, A.; Tamura, K.; Kinoshita, M.; Ichinose, T.; Nitta, H., Coarse particulate matter and emergency ambulance dispatches in Fukuoka, Japan: a time-stratified case-crossover study. *Environmental Health and Preventive Medicine* **2015**, *20*, (2), 130-136.
46. Michikawa, T.; Ueda, K.; Takeuchi, A.; Kinoshita, M.; Hayashi, H.; Ichinose, T.; Nitta, H., Impact of short-term exposure to fine particulate matter on emergency ambulance dispatches in Japan. *Journal of Epidemiology and Community Health* **2015**, *69*, (1), 86-91.
47. Milner, J.; Vardoulakis, S.; Chalabi, Z.; Wilkinson, P., Modelling inhalation exposure to combustion-related air pollutants in residential buildings: Application to health impact assessment. *Environment International* **2011**, *37*, (1), 268-279.
48. Mirabelli, M. C.; Vaidyanathan, A.; Flanders, W. D.; Qin, X. T.; Garbe, P., Outdoor PM_{2.5}, Ambient Air Temperature, and Asthma Symptoms in the Past 14 Days among Adults with Active Asthma. *Environmental Health Perspectives* **2016**, *124*, (12), 1882-1890.
49. Olaniyan, T. A.; Dalvie, M. A.; Roosli, M.; Jeebhay, M. F., AIR POLLUTION, POLLENS AND CHILDHOOD ASTHMA - IS THERE A LINK? *Current Allergy & Clinical Immunology* **2016**, *29*, (4), 252-261.
50. O'Neill, M. S.; Veves, A.; Zanobetti, A.; Sarnat, J. A.; Gold, D. R.; Economides, P. A.; Horton, E. S.; Schwartz, J., Diabetes enhances vulnerability to particulate air pollution - Associated impairment in vascular reactivity and endothelial function. *Circulation* **2005**, *111*, (22), 2913-2920.
51. Ostro, B.; Broadwin, R.; Green, S.; Feng, W. Y.; Lipsett, M., Fine particulate air pollution and mortality in nine California counties: Results from CALFINE. *Environmental Health Perspectives* **2006**, *114*, (1), 29-33.
52. Pope, C. A.; Rodermund, D. L.; Gee, M. M., Mortality effects of a copper smelter strike and reduced ambient sulfate particulate matter air pollution. *Environmental Health Perspectives* **2007**, *115*, (5), 679-683.
53. Rich, D. Q., Accountability studies of air pollution and health effects: lessons learned and recommendations for future natural experiment opportunities. *Environment International* **2017**, *100*, 62-78.
54. Ristovski, Z. D.; Miljevic, B.; Surawski, N. C.; Morawska, L.; Fong, K. M.; Goh, F.; Yang, I. A., Respiratory health effects of diesel particulate matter. *Respirology* **2012**, *17*, (2), 201-212.
55. Schwartz, J.; Coull, B.; Laden, F.; Ryan, L., The effect of dose and timing of dose on the association between airborne particles and survival. *Environmental Health Perspectives* **2008**, *116*, (1), 64-69.
56. Schwartz, J.; Bind, M. A.; Koutrakis, P., Estimating Causal Effects of Local Air Pollution on Daily Deaths: Effect of Low Levels. *Environmental Health Perspectives* **2017**, *125*, (1), 23-29.
57. Shaddick, G.; Lee, D.; Wakefield, J., Ecological bias in studies of the short-term effects of air pollution on health. *International Journal of Applied Earth Observation and Geoinformation* **2013**, *22*, 65-74.

58. Shi, L. H.; Zanobetti, A.; Kloog, I.; Coull, B. A.; Koutrakis, P.; Melly, S. J.; Schwartz, J. D., Low-Concentration PM_{2.5} and Mortality: Estimating Acute and Chronic Effects in a Population-Based Study. *Environmental Health Perspectives* **2016**, *124*, (1), 46-52.
59. Veras, M. M.; Alves, N. D.; Fajersztajn, L.; Saldiva, P., Before the first breath: prenatal exposures to air pollution and lung development. *Cell and Tissue Research* **2017**, *367*, (3), 445-455.
60. Wang, R.; Xiao, X.; Shen, Z. X.; Cao, L.; Cao, Y. X., Airborne fine particulate matter causes murine bronchial hyperreactivity via MAPK pathway-mediated M-3 muscarinic receptor upregulation. *Environmental Toxicology* **2017**, *32*, (2), 371-381.
61. Zanobetti, A.; Schwartz, J.; Samoli, E.; Gryparis, A.; Touloumi, G.; Peacock, J.; Anderson, R. H.; Le Tertre, A.; Bobros, J.; Celko, M.; Goren, A.; Forsberg, B.; Michelozzi, P.; Rabczenko, D.; Hoyos, S. P.; Wichmann, H. E.; Katsouyanni, K., The temporal pattern of respiratory and heart disease mortality in response to air pollution. *Environmental Health Perspectives* **2003**, *111*, (9), 1188-1193.
62. Sarnat, J. A.; Holguin, F., Asthma and air quality. *Current Opinion in Pulmonary Medicine* **2007**, *13*, (1), 63-66.
63. Gass, K.; Balachandran, S.; Chang, H. H.; Russell, A. G.; Strickland, M. J., Ensemble-Based Source Apportionment of Fine Particulate Matter and Emergency Department Visits for Pediatric Asthma. *American Journal of Epidemiology* **2015**, *181*, (7), 504-512.
64. Ballesta, P. P.; Field, R. A.; Fernandez-Patier, R.; Madruga, D. G.; Connolly, R.; Caracena, A. B.; De Saeger, E., An approach for the evaluation of exposure patterns of urban populations to air pollution. *Atmospheric Environment* **2008**, *42*, (21), 5350-5364.
65. Broich, A. V.; Gerharz, L. E.; Klemm, O., Personal monitoring of exposure to particulate matter with a high temporal resolution. *Environmental Science and Pollution Research* **2012**, *19*, (7), 2959-2972.
66. Halios, C. H.; Helmis, C. G., Temporal evolution of the main processes that control indoor pollution in an office microenvironment: a case study. *Environmental Monitoring and Assessment* **2010**, *167*, (1-4), 199-217.
67. Kadiyala, A.; Kumar, A., Multivariate Time Series Models for Prediction of Air Quality Inside a Public Transportation Bus Using Available Software. *Environmental Progress & Sustainable Energy* **2014**, *33*, (2), 337-341.
68. Mohammadyan, M., Determinants of Personal Exposure to PM_{2.5} in Office Workers. *Indoor and Built Environment* **2012**, *21*, (5), 710-717.
69. Reddy, A. L.; Gomez, M.; Dixon, S. L., The New York State Healthy Neighborhoods Program: Findings From an Evaluation of a Large-Scale, Multisite, State-Funded Healthy Homes Program. *Journal of Public Health Management and Practice* **2017**, *23*, (2), 210-218.
70. Vu, T. V.; Ondracek, J.; Zdimal, V.; Schwarz, J.; Delgado-Saborit, J. M.; Harrison, R. M., Physical properties and lung deposition of particles emitted from five major indoor sources. *Air Quality Atmosphere and Health* **2017**, *10*, (1), 1-14.
71. Dadvand, P.; de Nazelle, A.; Triguero-Mas, M.; Schembari, A.; Cirach, M.; Amoly, E.; Figueras, F.; Basagana, X.; Ostro, B.; Nieuwenhuijsen, M., Surrounding

- Greenness and Exposure to Air Pollution During Pregnancy: An Analysis of Personal Monitoring Data. *Environmental Health Perspectives* **2012**, *120*, (9), 1286-1290.
72. Canha, N.; Almeida, S. M.; Freitas, M. D.; Wolterbeek, H. T., Assessment of bioaerosols in urban and rural primary schools using passive and active sampling methodologies. *Archives of Environmental Protection* **2015**, *41*, (4), 11-22.
73. Alam, K.; Shaheen, K.; Blaschke, T.; Chishtie, F.; Khan, H. U.; Haq, B. S., Classification of Aerosols in an Urban Environment on the Basis of Optical Measurements. *Aerosol and Air Quality Research* **2016**, *16*, (10), 2535-2549.
74. Bluvshstein, N.; Flores, J. M.; Segev, L.; Rudich, Y., A new approach for retrieving the UV-vis optical properties of ambient aerosols. *Atmospheric Measurement Techniques* **2016**, *9*, (8), 3477-3490.
75. Panchenko, M. V.; Sviridenkov, M. A.; Terpugova, S. A.; Kozlov, V. S., Active spectral nephelometry as a method for the study of submicron atmospheric aerosols. *International Journal of Remote Sensing* **2008**, *29*, (9), 2567-2583.
76. Onasch, T. B.; Massoli, P.; Kebedian, P. L.; Hills, F. B.; Bacon, F. W.; Freedman, A., Single Scattering Albedo Monitor for Airborne Particulates. *Aerosol Science and Technology* **2015**, *49*, (4), 267-279.
77. Lambe, A. T.; Cappa, C. D.; Massoli, P.; Onasch, T. B.; Forestieri, S. D.; Martin, A. T.; Cummings, M. J.; Croasdale, D. R.; Brune, W. H.; Worsnop, D. R.; Davidovits, P., Relationship between Oxidation Level and Optical Properties of Secondary Organic Aerosol. *Environmental Science & Technology* **2013**, *47*, (12), 6349-6357.
78. Cappa, C. D.; Che, D. L.; Kessler, S. H.; Kroll, J. H.; Wilson, K. R., Variations in organic aerosol optical and hygroscopic properties upon heterogeneous OH oxidation. *Journal of Geophysical Research-Atmospheres* **2011**, *116*.
79. Petzold, A.; Rasp, K.; Weinzierl, B.; Esselborn, M.; Hamburger, T.; Dornbrack, A.; Kandler, K.; Schutz, L.; Knippertz, P.; Fiebig, M.; Virkkula, A., Saharan dust absorption and refractive index from aircraft-based observations during SAMUM 2006. *Tellus Series B-Chemical and Physical Meteorology* **2009**, *61*, (1), 118-130.
80. Laven, P. MiePlot: A computer program for scattering of light from a sphere using Mie theory & the Debye series. <http://www.philiplaven.com/mieplot.htm>
81. Esteve, A. R.; Estelles, V.; Utrillas, M. P.; Martinez-Lozano, J. A., In-situ integrating nephelometer measurements of the scattering properties of atmospheric aerosols at an urban coastal site in western Mediterranean. *Atmospheric Environment* **2012**, *47*, 43-50.
82. Balakrishnaiah, G.; Kumar, K. R.; Reddy, B. S. K.; Gopal, K. R.; Reddy, R. R.; Reddy, L. S. S.; Ahammed, Y. N.; Narasimhulu, K.; Moorthy, K. K.; Babu, S. S., Analysis of optical properties of atmospheric aerosols inferred from spectral AODs and Angstrom wavelength exponent. *Atmospheric Environment* **2011**, *45*, (6), 1275-1285.
83. Bibi, S.; Alam, K.; Chishtie, F.; Bibi, H., Characterization of absorbing aerosol types using ground and satellites based observations over an urban environment. *Atmospheric Environment* **2017**, *150*, 126-135.
84. Rajasegarar, S.; Havens, T. C.; Karunasekera, S.; Leckie, C.; Bezdek, J. C.; Jamriska, M.; Gunatilaka, A.; Skvortsov, A.; Palaniswami, M., High-Resolution

- Monitoring of Atmospheric Pollutants Using a System of Low-Cost Sensors. *Ieee Transactions on Geoscience and Remote Sensing* **2014**, *52*, (7), 3823-3832.
85. Castell, N.; Dauge, F. R.; Schneider, P.; Vogt, M.; Lerner, U.; Fishbain, B.; Broday, D.; Bartonova, A., Can commercial low-cost sensor platforms contribute to air quality monitoring and exposure estimates? *Environment International* **2017**, *99*, 293-302.
86. Gao, M. L.; Cao, J. J.; Seto, E., A distributed network of low-cost continuous reading sensors to measure spatiotemporal variations of PM_{2.5} in Xi'an, China. *Environmental Pollution* **2015**, *199*, 56-65.
87. Jiao, W.; Hagler, G.; Williams, R.; Sharpe, R.; Brown, R.; Garver, D.; Judge, R.; Caudill, M.; Rickard, J.; Davis, M.; Weinstock, L.; Zimmer-Dauphinee, S.; Buckley, K., Community Air Sensor Network (CAIRSENSE) project: evaluation of low-cost sensor performance in a suburban environment in the southeastern United States. *Atmospheric Measurement Techniques* **2016**, *9*, (11), 5281-5292.
88. Manikonda, A.; Zikova, N.; Hopke, P. K.; Ferro, A. R., Laboratory assessment of low-cost PM monitors. *Journal of Aerosol Science* **2016**, *102*, 29-40.
89. Sousan, S.; Koehler, K.; Thomas, G.; Park, J. H.; Hillman, M.; Halterman, A.; Peters, T. M., Inter-comparison of low-cost sensors for measuring the mass concentration of occupational aerosols. *Aerosol Science and Technology* **2016**, *50*, (5), 462-473.
90. Kelly, K. E.; Whitaker, J.; Petty, A.; Widmer, C.; Dybwad, A.; Sleeth, D.; Martin, R.; Butterfield, A., Ambient and laboratory evaluation of a low-cost particulate matter sensor. *Environmental Pollution* **2017**, *221*, 491-500.
91. Maricq, M. M., Monitoring Motor Vehicle PM Emissions: An Evaluation of Three Portable Low-Cost Aerosol Instruments. *Aerosol Science and Technology* **2013**, *47*, (5), 564-573.
92. Palacios-Pena, L.; Baro, R.; Guerrero-Rascado, J. L.; Alados-Arboledas, L.; Brunner, D.; Jimenez-Guerrero, P., Evaluating the representation of aerosol optical properties using an online coupled model over the Iberian Peninsula. *Atmospheric Chemistry and Physics* **2017**, *17*, (1), 277-296.
93. Patel, S.; Li, J. Y.; Pandey, A.; Pervez, S.; Chakrabarty, R. K.; Biswas, P., Spatio-temporal measurement of indoor particulate matter concentrations using a wireless network of low-cost sensors in households using solid fuels. *Environmental Research* **2017**, *152*, 59-65.
94. Piedrahita, R.; Xiang, Y.; Masson, N.; Ortega, J.; Collier, A.; Jiang, Y.; Li, K.; Dick, R. P.; Lv, Q.; Hannigan, M.; Shang, L., The next generation of low-cost personal air quality sensors for quantitative exposure monitoring. *Atmospheric Measurement Techniques* **2014**, *7*, (10), 3325-3336.
95. Semple, S.; Ibrahim, A. E.; Apsley, A.; Steiner, M.; Turner, S., Using a new, low-cost air quality sensor to quantify second-hand smoke (SHS) levels in homes. *Tobacco Control* **2015**, *24*, (2), 153-158.
96. Cheng, Y.; Li, X.; Li, Z.; Jiang, S.; Li, Y.; Jia, J.; Jiang, X., AirCloud: a cloud-based air-quality monitoring system for everyone. In *Proceedings of the 12th ACM Conference on Embedded Network Sensor Systems*, ACM: Memphis, Tennessee, 2014; pp 251-265.

97. Sousan, S.; Koehler, K.; Hallett, L.; Peters, T. M., Evaluation of the Alphasense optical particle counter (OPC-N2) and the Grimm portable aerosol spectrometer (PAS-1.108). *Aerosol Science and Technology* **2016**, *50*, (12), 1352-1365.
98. Johnson, K. K.; Bergin, M. H.; Russell, A. G.; Hagler, G. S. W., Using Low Cost Sensors to Measure Ambient Particulate Matter Concentrations and On-Road Emissions Factors. *Atmospheric Measurement Techniques Discussion* **2016**.
99. Bischof, O. F. H., Hans-Georg, Operation Recommendations for the Model 3076 Constant Output Atomizer. In TSI Incorporated: 2000.
100. Hayati, A.; Mattsson, M.; Sandberg, M., Single-sided ventilation through external doors: Measurements and model evaluation in five historical churches. *Energy and Buildings* **2017**, *141*, 114-124.
101. Habre, R.; Coull, B.; Moshier, E.; Godbold, J.; Grunin, A.; Nath, A.; Castro, W.; Schachter, N.; Rohr, A.; Kattan, M.; Spengler, J.; Koutrakis, P., Sources of indoor air pollution in New York City residences of asthmatic children. *Journal of Exposure Science and Environmental Epidemiology* **2014**, *24*, (3), 269-278.
102. Tang, I. N., Chemical and size effects of hygroscopic aerosols on light scattering coefficients. *Journal of Geophysical Research-Atmospheres* **1996**, *101*, (D14), 19245-19250.
103. Bartington, S. E.; Bakolis, I.; Devakumar, D.; Kurmi, O. P.; Gulliver, J.; Chaube, G.; Manandhar, D. S.; Saville, N. M.; Costello, A.; Osrin, D.; Hansell, A. L.; Ayres, J. G., Patterns of domestic exposure to carbon monoxide and particulate matter in households using biomass fuel in Janakpur, Nepal. *Environmental Pollution* **2017**, *220*, 38-45.
104. Maskova, L.; Smolik, J.; Travnickova, T.; Havlica, J.; Ondrackova, L.; Ondracek, J., Contribution of Visitors to the Indoor PM in the National Library in Prague, Czech Republic. *Aerosol and Air Quality Research* **2016**, *16*, (7), 1713-1721.
105. Muindi, K.; Kimani-Murage, E.; Egondi, T.; Rocklov, J.; Ng, N., Household Air Pollution: Sources and Exposure Levels to Fine Particulate Matter in Nairobi Slums. *Toxics* **2016**, *4*, (3).
106. Zhou, Z. H.; Liu, Y. R.; Yuan, J. J.; Zuo, J.; Chen, G. Y.; Xu, L. Y.; Rameezdeen, R., Indoor PM_{2.5} concentrations in residential buildings during a severely polluted winter: A case study in Tianjin, China. *Renewable & Sustainable Energy Reviews* **2016**, *64*, 372-381.
107. Zhu, Y.; Smith, T. J.; Davis, M. E.; Levy, J. I.; Herrick, R.; Jiang, H. Y., Comparing Gravimetric and Real-Time Sampling of PM_{2.5} Concentrations Inside Truck Cabins. *Journal of Occupational and Environmental Hygiene* **2011**, *8*, (11), 662-672.
108. Cambra-Lopez, M.; Winkel, A.; Mosquera, J.; Ogink, N. W. M.; Aarnink, A. J. A., Comparison between light scattering and gravimetric samplers for PM₁₀ mass concentration in poultry and pig houses. *Atmospheric Environment* **2015**, *111*, 20-27.
109. Viana, M.; Rivas, I.; Reche, C.; Fonseca, A. S.; Perez, N.; Querol, X.; Alastuey, A.; Alvarez-Pedrerol, M.; Sunyer, J., Field comparison of portable and

- stationary instruments for outdoor urban air exposure assessments. *Atmospheric Environment* **2015**, *123*, 220-228.
110. Wang, Z. C.; Calderon, L.; Patton, A. P.; Allacci, M. S.; Senick, J.; Wener, R.; Andrews, C. J.; Mainelis, G., Comparison of real-time instruments and gravimetric method when measuring particulate matter in a residential building. *Journal of the Air & Waste Management Association* **2016**, *66*, (11), 1109-1120.
111. Lung, S. C. C.; Hu, S. C., Generation rates and emission factors of particulate matter and particle-bound polycyclic aromatic hydrocarbons of incense sticks. *Chemosphere* **2003**, *50*, (5), 673-679.
112. Stubbs, C. W.; Doherty, P.; Cramer, C.; Narayan, G.; Brown, Y. J.; Lykke, K. R.; Woodward, J. T.; Tonry, J. L., PRECISE THROUGHPUT DETERMINATION OF THE PanSTARRS TELESCOPE AND THE GIGAPIXEL IMAGER USING A CALIBRATED SILICON PHOTODIODE AND A TUNABLE LASER: INITIAL RESULTS. *Astrophysical Journal Supplement Series* **2010**, *191*, (2), 376-388.
113. Linke, C.; Ibrahim, I.; Schleicher, N.; Hitzenberger, R.; Andreae, M. O.; Leisner, T.; Schnaiter, M., A novel single-cavity three-wavelength photoacoustic spectrometer for atmospheric aerosol research. *Atmospheric Measurement Techniques* **2016**, *9*, (11), 5331-5346.
114. Skoog, D. A.; Holler, F. J.; Crouch, S. R., *Principles of instrumental analysis*. Brooks/Cole : Thomson Learning: Australia, 2007.
115. Voigtman, E., Comparison of Signal-to-Noise Ratios. *Analytical Chemistry* **1997**, *69*, (2), 226-234.
116. Williams, R.; Kaufman, A.; Hanley, T.; Rice, J.; Garvey, S., Evaluation of Field-deployed Low Cost PM Sensors. In Agency, E. P., Ed. EPA: Washington, DC, 2014; Vol. 600.
117. Novosselov, I. V.; Ariessohn, P. C., Rectangular Slit Atmospheric Pressure Aerodynamic Lens Aerosol Concentrator. *Aerosol Science and Technology* **2014**, *48*, (2), 163-172.

